A Breathing Stabilization System

A thesis submitted in fulfilment

of the requirements of the degree of

Master of Engineering

at the

University of Waikato

by

Heping (Harry) Ling

2008

ACKNOWLEDGEMENTS

I would like to thank and acknowledge the support and assistance of the following people and groups who contributed to this project.

I would like to thank Howell Round, not only for his expertise and the constructive advice he imparted, but for the many hours of his time that he spent assisting me. Also for the fact that he was always available to hear and make comment on my ideas and to keep me in check if I tried to take on too much.

Many thanks to Jonathan who was giving me much assistance for the power electronics part. Thanks also for advice and ideas on the development of this thesis.

A big thank you to Stuart for prompting me to take a different perspective on various aspects of my work, and for continually asking for the reasons behind decisions made in this research.

Thank you to Michael for his thought and advice on identifying a valuable research direction and for providing many innovative ideas and solutions in this research. Thanks also to who always responded to my many requests for components.

An expression of gratitude also goes to those people in the lab who provided valuable insight into this research.

Lastly, specially thanks for my kindly parents and my girlfriend Lin Han.

ABSTRACT

Breathing Stabilization System is a new idea and method. The purpose of this system is to produce a device to control a patient's breathing for gated radiotherapy.

This thesis focuses on building a simple Breathing Stabilization System that includes five solenoids, a power supply and five force sensors to build up the whole system.

Significantly, this thesis will introduce the modeling of solenoids in detail that include how to build a mathematical model of the solenoids. The simulation of the electromagnetic in professional multi-physics software COMSOL will also be explained.

To drive the solenoid system, a voltage-to-current converter is used. This part will be introduced as well as the operational amplifier circuit used by the force sensors.

CONTENTS

LIST OF FIGURES

LIST OF TABLES

1 INTRODUCTION

1.1 Background

Radiotherapy is a local radiation treatment that is designed to treat the defined tumour and spare the surrounding normal tissue from receiving radiation doses above specified dose tolerances. There are many factors that may contribute to differences between the planned dose distribution and the delivered dose distribution. One such factor is uncertainty in patient position on the treatment unit. [1]

Image-guided radiotherapy (IGRT) is the process of frequent two and three-dimensional imaging, during a course of radiation treatment, used to direct radiotherapy utilizing the imaging coordinates of the actual radiation treatment plan. The patient is localized in the treatment room in the same position as planned from the reference imaging dataset. Three-dimensional (3D) IGRT would include localization of a cone-beam computed tomography (CBCT) dataset with the planning computed tomography (CT) dataset from planning for example. Two-dimensional (2D) IGRT would include matching planar kilo-voltage (kV) radiographs fluoroscopy or megavoltage (MV) images with digital reconstructed radiographs (DRRs) from the planning CT.

This process is distinct from the use of imaging to delineate targets and organs in

the planning process of radiation therapy. However, there is clearly a connection between the imaging processes as IGRT relies directly on the imaging modalities from planning as the reference coordinates for localizing the patient. The variety of image gathering hardware used in planning includes Computed Tomography (CT), Magnetic Resonance Imaging (MRI), and Positron Emission Tomography (PET) among others. Through advancements in imaging technology, combined with a further understanding of human biology at the molecular level, the impact of IGRT on radiotherapy treatment continues to evolve. [2]

Numerous advances in radiotherapy have been achieved in recent years. By using image-guided radiotherapy, with or without intensity modulation, it is now possible to match the irradiation volume to the shape of the tumor and so better preserve neighboring healthy tissue.

Now some institutes are taking up a new technological challenge with the treatment of the patients by also using gated radiotherapy. Radiotherapists face particular problems in the chest area (lungs, breasts, etc) since the tumors move during breathing. Through the development of gated radiotherapy, tumor motion can now be taken into account very precisely.

Respiratory gating is used to counter the effects of organ motion during radiotherapy for chest tumors. With this technique, radiation is only applied when

the tumour moves into position in the treatment beam. The effects of variations in patient breathing patterns during a single treatment and from day to day are unknown. Researchers have evaluated the feasibility of using patient training tools and their effect on the breathing cycle regularity and reproducibility during respiratory-gated radiotherapy. If the breathing is regular, then the gating can be done more accurately. To monitor respiratory patterns, they used a component of a commercially available respiratory-gated radiotherapy system. The passive marker video tracking system consists of reflective markers placed on the patient's chest or abdomen, which are detected by a wall-mounted video camera. Software installed on a PC interfaced to this camera detects the marker motion digitally and records it. The marker position as a function of time serves as the motion signal that may be used to trigger imaging or treatment. The training tools used were audio prompting and visual feedback, with free breathing as a control. The audio prompting method used instructions to "breathe in" or "breathe out" at periodic intervals deduced from patients' own breathing patterns. In the visual feedback method, patients were shown a real-time trace of their abdominal wall motion due to breathing. Using this, they were asked to maintain a constant amplitude of motion. Motion traces of the abdominal wall were recorded for each patient for various maneuvers. Free breathing showed a variable amplitude and frequency. Audio prompting resulted in a reproducible frequency; however, the variability and the magnitude of amplitude increased. Visual feedback gave a better control over the amplitude but showed minor variations in frequency. They

concluded that training improves the reproducibility of amplitude and frequency of patient breathing cycles. This may increase the accuracy of respiratory-gated radiotherapy. [3]

The current methods that have been described above require patient co-operation. Now the system we want to design will periodically provide a tactile signal for the patient to synchronize their breathing to. The method has two advantages: firstly, it should induce a more consistent breathing pattern and secondly, it may not require patient co-operation.

1.2 Aim of the project

This thesis describes the construction of a low-cost, simple Breathing Stabilization System. The purpose of this is to produce a device to control a patient's breathing for gated radiotherapy.

To achieve this purpose, it was proposed to construct a system to squeeze the abdomen under computer control. The system is to consist of several solenoids strapped across the abdomen. A force sensor is to be mounted on the top of each solenoid to monitor the force applied to the abdomen by each solenoid. This feedback system can be implemented to provide full control over the force applied by each solenoid.

1.3 Thesis structure

This thesis focuses on how to build a simple Breathing Stabilization System.

Chapter 2 presents the modeling of the system.

Chapter 3 covers the circuits design that including the driver system (voltage-to-current converter) and operational amplifier circuit for force sensor.

In *Chapter 4*, we will describe testing of the system.

Chapter 5 discusses how the system can be developed further.

2 THE SOLENOID SYSTEM

2.1 Description of the system

The project we intended to build is a prototype electromechanical system for periodically compressing the abdomen to provide a tactile signal for a patient to synchronise to and thus stabilise their breathing. The method we proposed is to:

1 Squeeze the abdomen in a rhythmic pattern to provide a tactile signal using a solenoid system.

2 Detect the force applied to monitor the tactile signal.

3 Adjust the applied force during the compression to provide the appropriate tactile signal.

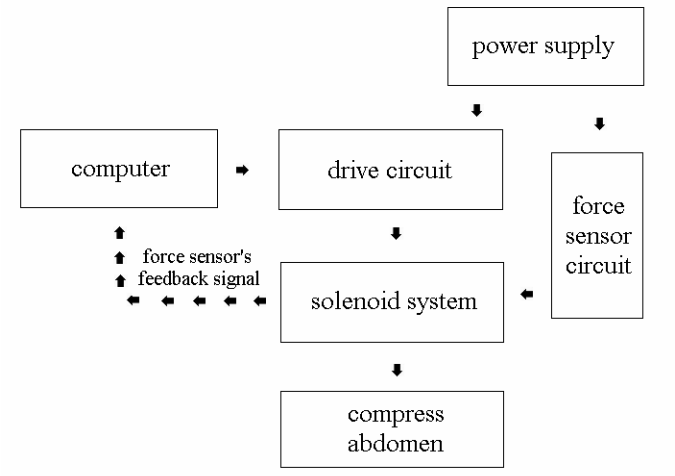

Figure 2-1 Whole system schematic

The whole system is shown in *Fig 2.1*. The solenoid system is controlled via a drive circuit by a computer. The computer provides a 0 V-5 V output which is converted to current by the drive circuit, and is then input to the solenoid system.

So the force applied to the abdomen is dependent on the computer control. The force sensor circuit converts the force (tactile signal) produced by solenoid system to an electrical signal, which is sent to the computer. Based on the feedback signal provided by force sensor, the computer can adjust the applied force.

A person wearing the solenoid system is shown in *Fig 2.2*.

Figure 2-2 View of person wearing the solenoid system

The solenoid system is shown in *Fig 2.3*. In order to strap the five solenoids across the abdomen, a belt is used with five plastic boards onto which the solenoids are attached.

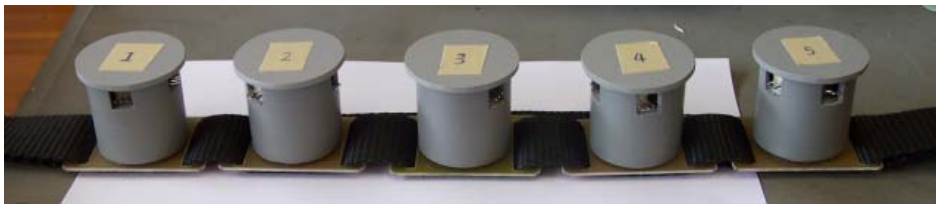

Figure 2-3 The solenoid system

Each solenoid consists of a steel cylindrical case with a permanent magnet mounted inside *(Fig 2.4)* and an aluminium bobbin onto which a coil is wound *(Fig 2.5)*.

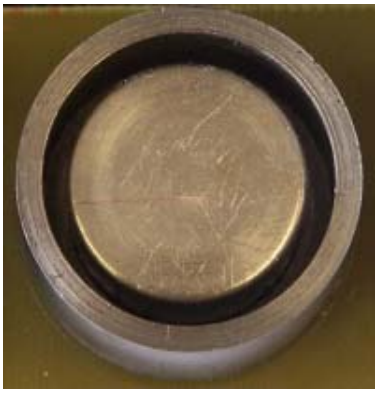

Figure 2-4 Steel cylindrical case with permanent magnet

The magnet has an outside diameter at 25 mm and a height of 20 mm.

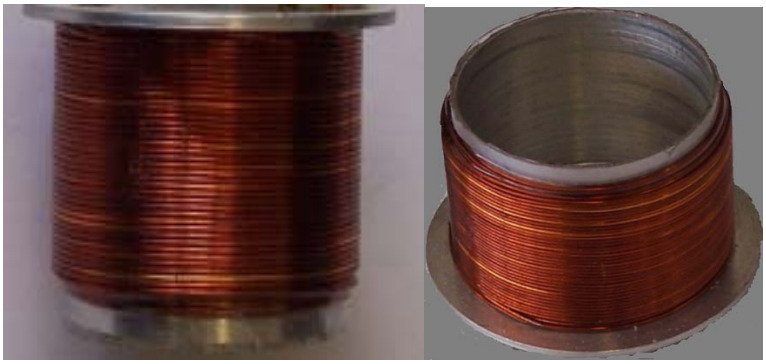

Figure 2-5 Aluminium bobbin with coil

The bobbin fits down inside the cylinder in the gap between the magnet and the cylinder wall. The cylinder is shown in cross-section in *Fig 2.6*.

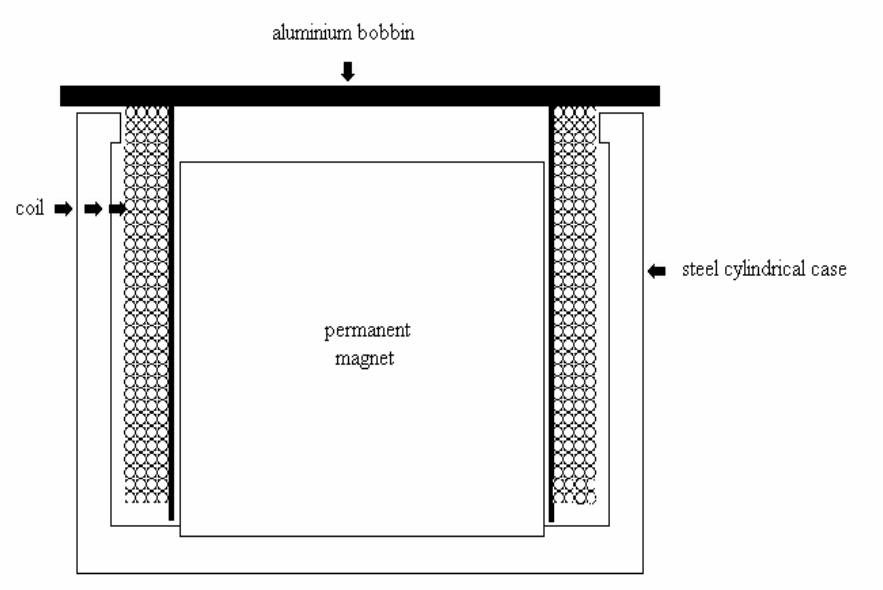

Figure 2-6 The structure of the solenoid

The geometry of solenoid is sketched in *Fig 2.6*. The permanent magnet and steel cylindrical case establishes a radial field in the cylindrical gap between the top of the cylinder and the magnet. When a current is flows in the coil wound on the aluminium bobbin, a force results which causes the aluminium bobbin to move against the abdomen. The material of cap and cylinder must be chosen carefully. In order to find ideal dimensions for the solenoid system, a simulation in COMSOL Multi-physics software was done.

There are two factors affect the effect of whole system: one is the magnitude of

force applied to the abdomen, the other is the depth that solenoid squeeze the abdomen. To provide a satisfactory tactile signal a maximum force of 10 N should be provided by and the maximum bobbin movement should be about 10 mm. Two main problems need to be investigated: one is the sort and size of magnets to be used, the other is the best dimensions of the solenoid.

Neodymium magnets were chosen for their large magnetic fields. The height of the solenoid must be over 10 mm to get sufficient bobbin movement; to keep the system as light as possible the smaller outside diameter the better. Designs were done for four typical Neodymium permanent magnets.

Type	Outside diameter (mm)	Thickness (mm)
ND125125	12.5	12.5
ND2012	20	12
ND2520	25	20
ND3510	35	10

Table 2-1 Dimensions of four types of magnet

The COMSOL multi-physics software showed that the solenoid system could produce the biggest force (over 10 N) when using ND2520 magnets. The magnetic parameters of ND2520 are displayed in the follow table:

B_r	1.200 T
μ_r	1.37
H	955 kA/m

Table 2-2 Magnetic parameters of ND2520

Here is the description of the dimensions of the solenoid system. The magnet's dimensions are: outside diameter is 25 mm; thickness is 20 mm. According to these parameters, we designed the dimensions of each part of the solenoid system from inside to outside. The first one is aluminium bobbin: the inside diameter is 25.6 mm that just a little bit bigger than the outside diameter of magnet, the gap (0.3 mm) between them is big enough to ensure there is a smooth movement when the aluminium bobbin goes up and down. The wall of aluminium bobbin's thickness is 0.2 mm; the height is 22.25 mm, the top part's thickness is 1 mm, which is strong enough to withstand the force applied to abdomen. Four layers of 55 turns of copper wire are wound on the aluminium bobbin. The diameter of the wire is 0.35 mm (our expected maximum current is 2 A that can safely flow in the wire). So the thickness of the coil is 1.4 mm. The outside diameter of aluminium bobbin with coil is 28.8 mm. The last part is the steel cylindrical case, the dimensions is shown in *Fig 2.7*.

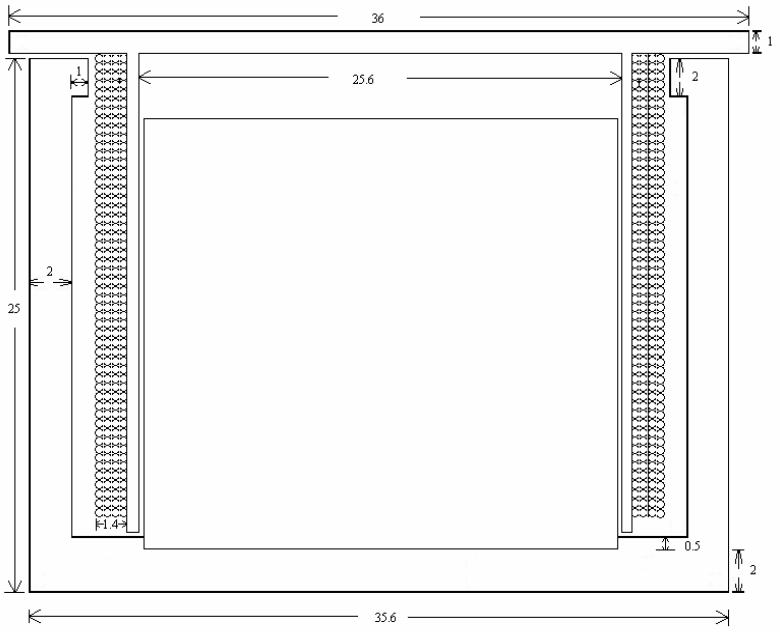

Figure 2-7 The dimensions of solenoid system

(All dimensions in mm)

The full design procedure is detailed in Appendix. This was used in the COMSOL model. Details of the modelling are given in Appendix. The COMSOL simulation of this system provided the data graphed in *Fig 2.8.*

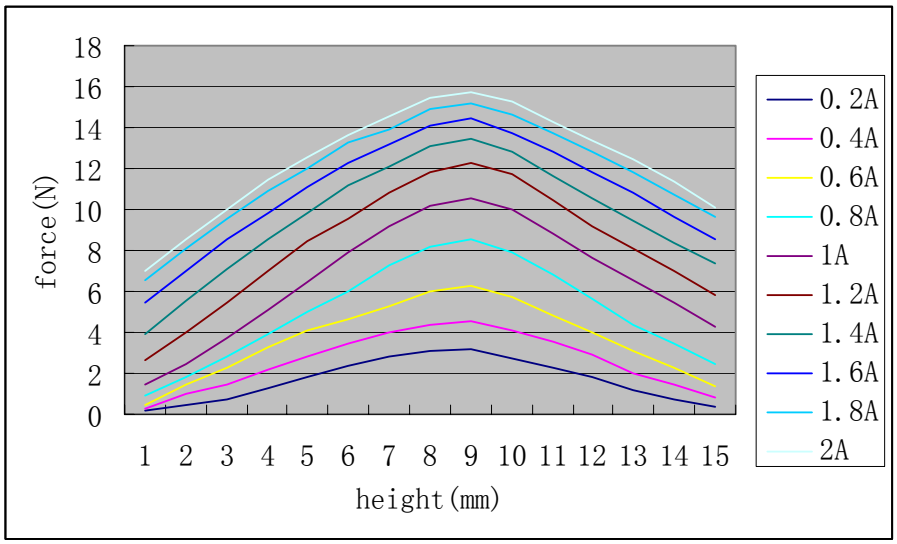

Figure 2-8 Simulation data

This data showed that a sufficient force can be obtained on that the force is relatively constant for all displacements of the solenoid bobbin.

2.2 Mathematical model of systems

Electric current and magnetic fields interact in many ways, some of which are important to gaining an understanding of the operation of most electromechanical energy conversion devices such as linear motors.

Mechanical Equations:

The electromagnetic effect of interest to us is the fact that a charge *q* moving with vector velocity $\vec{v}$ in a magnetic field of intensity $\vec{B}$ experiences a force $\vec{F}$ given by the vector cross-product $\vec{F} = q\vec{v} \times \vec{B}$ If the moving charge is composed of a current of *i* amperes in a conductor of length *l* meters arranged at right angles to the field strength of *B*, then the force at right angle to the plane of *i* and *B* has the magnitude

$$F = Bli \qquad \textit{(Eq. 2.1)}$$

This equation is the basis of using a magnetic field to convert electric energy from the source of current *i* into mechanical object. Such devices are called motors, and Eq 2.1 is called the Law of Motors.

The geometry we designed is the permanent magnet and steel cylindrical case establish a radial field in the cylindrical gap between them. When a current is caused to flow in the coil wound on the aluminium bobbin, the force causes the

aluminium bobbin to move against the abdomen.

If we approximate the effects of the air as if the abdomen had equivalent mass *M* and viscous damping coefficient *d*, then we can write the equations of motion of the device. The magnet establishes a uniform field of 1.2 T (that's up to the magnet we have chosen) and the coil has four layers of 55 turns at 25 mm diameter. The current is at right angles to the field, and the force of interest is at right angles to the plane of *i* and *B*, so Eq 2.1 applies. In this case the parameter values are *B*=1.2 T and

$$l = 4 \times 55 \times \frac{2\pi \times 1.25}{100} = 17.27\ (m) \qquad \textit{(Eq. 2.2)}$$

Thus

$$F = 20.724 \times i\ (N) \qquad \textit{(Eq. 2.3)}$$

The mechanical equation is

$$M\ddot{x} + d\dot{x} = 20.724 \times i \qquad \textit{(Eq. 2.4)}$$

We apply a current to our solenoid in order to produce a displacement which creates the pressure to abdomen.

Converting the above equation to the Laplace domain:

$$20.724 i(s) = Ms^2 X(s) + dsX(s) \qquad \textit{(Eq. 2.5)}$$

Rearranging: $\dfrac{X(s)}{I(s)} = \dfrac{20.724}{Ms^2 + ds}$ *(Eq. 2.6)*

This is the transfer function between the current through the coil, and the displacement of the coil.

In block diagram form:

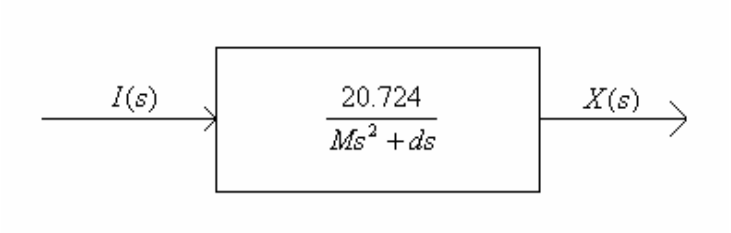

Figure 2-9 Block diagram

Electrical Equations:

In addition to Eq 2.1, which expresses force (a mechanical variable) in terms of current (an electrical variable), there is also a relation giving the effect of mechanical motion on electricity. The basic fact is that if a charge is moving in a magnetic field and is forced along a conductor, an electric voltage is established between the ends of the conductor. The relation is that if a conductor (which is filled with charged particles) of length l meters is moved at a velocity *v* meters or second through a constant field of *B* at right angles to the direction of the field, then the voltage between the ends of the conductor is given by

$$e(t) = Blv \qquad \textit{(Eq. 2.7)}$$

This expression is called the Law of Generator, for it is the basis for generating electric power by moving a conductor in a field and letting *e* cause current to flow in an external circuit. Considering again the situation of our project, we see that if motion results according to Eq 2.2, to create a current in the coil, must apply a voltage it. The coil forms an inductance in series with a resistance. A coil voltage V_{coil} gives rise to a current I, and by Ohm's law:

$$I = \frac{V_{coil}}{Z_{coil}} \qquad \textit{(Eq. 2.8)}$$

Where Z_{coil} is the impedance of the coil, given by:

$$Z_{coil} = sL + R \qquad \textit{(Eq. 2.9)}$$

The coil moving in a magnetic field, generates a back emf:

$$V_{emf} = Blv = Bl\dot{x} \qquad \textit{(Eq. 2.10)}$$

Because this voltage is opposite in sign to the applied voltage:

$$V_{applied} - V_{emf} = V_{coil} \qquad \textit{(Eq. 2.11)}$$

So

$$V_{coil} = V_{applied} - V_{emf} = V_{applied} - Bl\dot{x} \qquad \textit{(Eq. 2.12)}$$

Since

$$I = \frac{V_{coil}}{Z_{coil}} \qquad \textit{(Eq. 2.13)}$$

$$I = \frac{V_{applied} - Bl\dot{x}}{sL + R} = (V_{applied} - Bl\dot{x})\frac{1}{sL + R} \qquad \textit{(Eq. 2.14)}$$

Transforming to the Laplace domain:

$$I(s) = \left[V_{applied}(s) - BlsX(s)\right]\frac{1}{sL + R} \qquad \textit{(Eq. 2.15)}$$

This implies that the electrical characteristic consists of a linear system with two inputs (V_{applied} , X) and one output (I).

We could write this in block diagram form as:

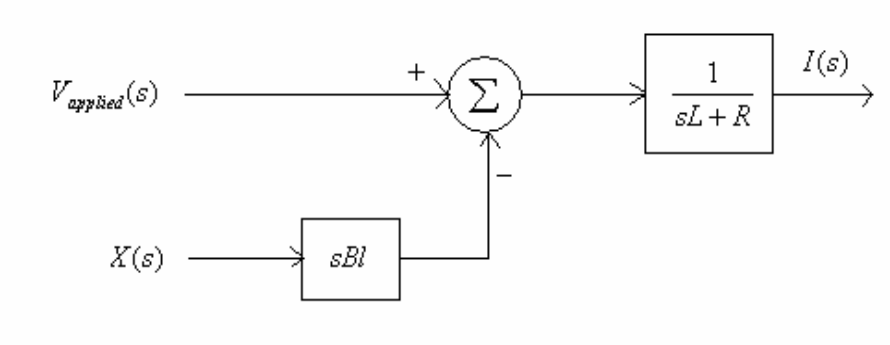

Figure 2-10 Transfer function I

So, in summary our mechanical equation is:

$$\frac{X(s)}{I(s)} = \frac{20.724}{Ms^2 + ds} \qquad \textit{(Eq. 2.16)}$$

And our electrical equation is:

$$I(s) = (V_{applied}(s) - BlsX(s))\frac{1}{sL+R} \qquad \textit{(Eq. 2.17)}$$

These can be solved simultaneously to give the result:

$$\frac{X(s)}{V_{applied}(s)} = \frac{20.724}{(20.724^2 + dR)s + (dL + MR)s^2 + LMS^3} \qquad \textit{(Eq. 2.18)}$$

The block diagrams for different parts of the system appear:

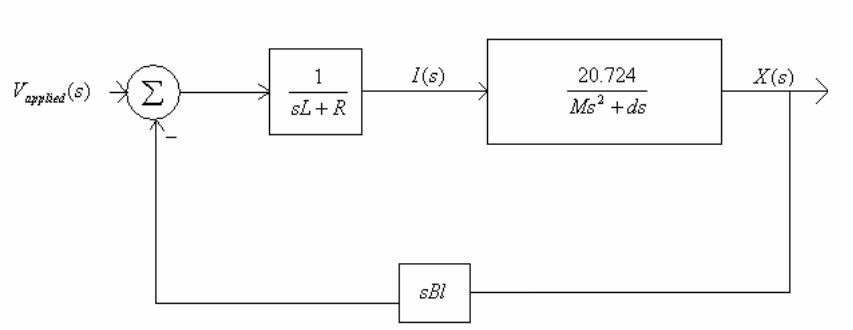

Figure 2-11 Transfer function II

3 CIRCUITS DESIGN

3.1 Drive circuit of solenoid system

To drive the solenoid system, a voltage-to-current converter was designed. The schematic diagram of the drive circuit is shown in *Fig 3.1*.

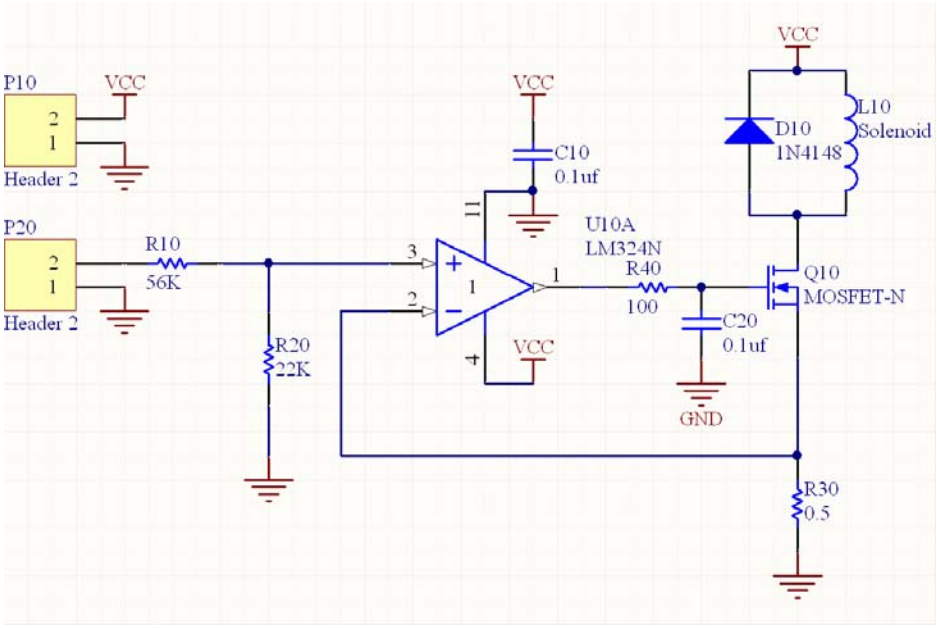

Figure 3-1 The drive circuit of Solenoid system

P20 is the port provided the 0 V- 5V by computer. In order to improve the accuracy and flexibility of the system, the circuit uses MOSFET to improve the control of the output current and to allow a larger range of output current to be obtained. The circuit is shown in *Fig 3.2*.

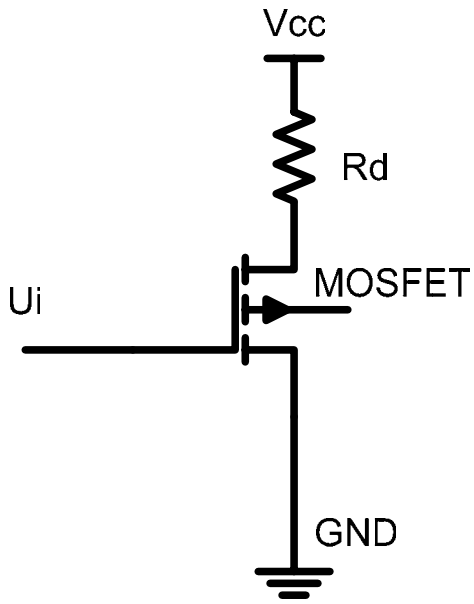

Figure 3-2 Solenoid system drive circuit's output part

The negative feedback of this operational amplifier is obtained from the upper terminal of R_{30}. The current change in R_{30}, which is also the current change of the MOSFET drain-source, reflects the current change of the load. This current change can be expressed as the voltage of R_{30}. To stabilize the change of the output current, the voltage of R_{30} is collected by the non-inverting terminal of the op amp to make up a closed loop.

There is a diode in parallel with the solenoid at the last stage of the circuit. This is to prevent damage to the MOSFET by the surge voltage from the power line. This diode is also named a freewheeling diode. Without this freewheeling diode, the inductive voltage at the moment of the solenoid switching off might blow the

MOSFET up.

The output voltage of the MOSFET is smoothed by the RC filter of R_{40} and C_{20}. It will make the MOSFET work in a more stable manner.

C_{10} is selected for filtering the power line noise and make the power supply of the op amp clean. It makes sure the whole system working in a good condition.

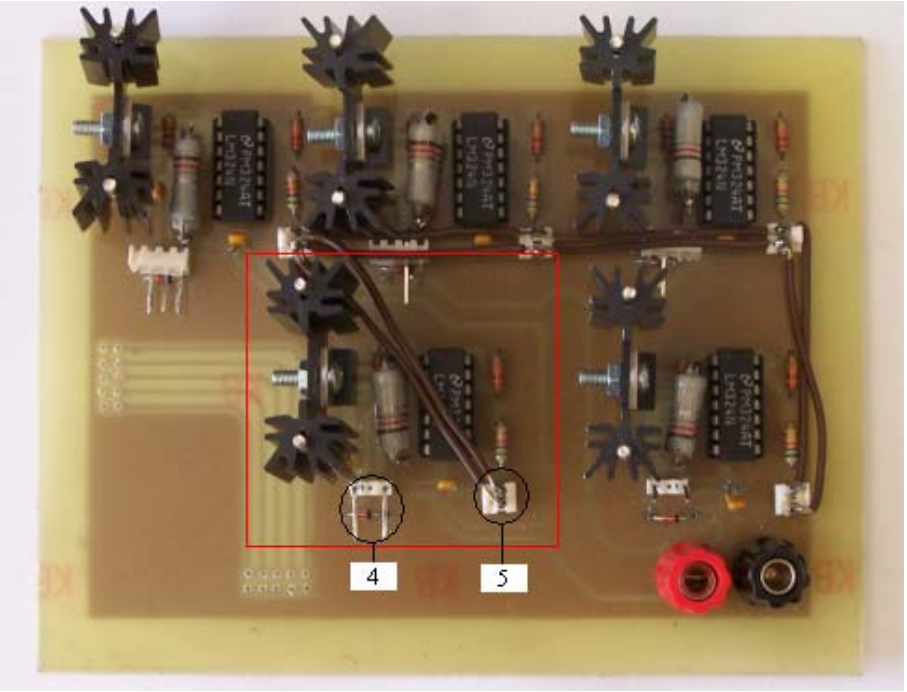

Figure 3-3 Drive circuit board

View of the drive circuit board is shown in *Fig 3.3*. One of the drive circuits is in the red rectangle area, the whole drive circuit board includes five of those. Port 4 is the solenoid system's power supply, Port 5 provides the 0 V- 5V from the computer.

3.2 The Force Sensor Circuit

The force between the solenoid and the abdomen is sensed by the circuit in *Fig 3.4.*

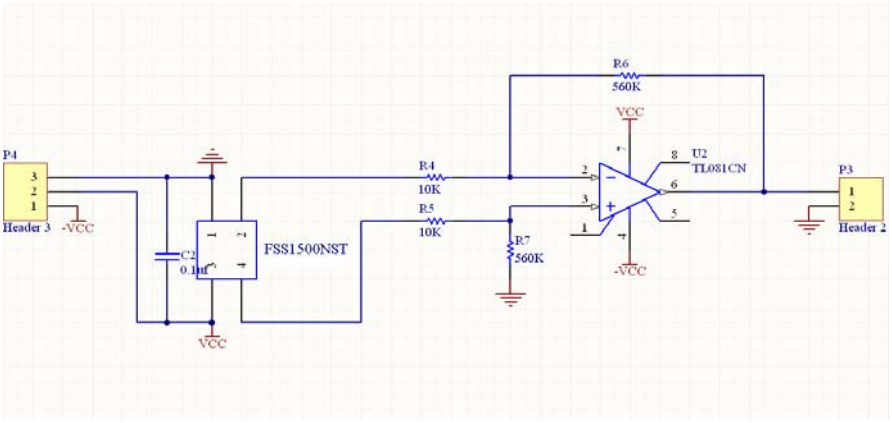

Figure 3-4 Force sensor circuit

As *Fig 3.4* shows, we were using Honeywell FSS1500NST force sensor. It operates on the principle that the resistance of silicon-implanted piezoresistors will increase when the resistors flex under any applied force. The sensor transmits force via a stainless steel ball in the sensor, directly to the silicon-sensing element. The amount of resistance changes in proportion to the amount of force being applied. This change in circuit resistance results in a corresponding mV output level change. A simple op amp circuit was used to amplify the force signal.

The TL081, it is a high speed J–FET input single operational amplifier incorporating well matched, high voltage J–FET and bipolar transistors in a monolithic integrated circuit. It has a large input resistance because of its low input bias and offset currents. It's suitable to work as the amplifier of this circuit.

The TL081 amplifier needs a bipolar power supply. We chose +5V and -5V.

In order to change the gains of the circuit, we can adjust the value of the resistance. The gain is depend on the value of R6 and R4,

$$V_0 = \frac{R6/R4}{U2 - U4} \qquad \textit{(Eq. 3.1)}$$

We have chosen R4 = R5 = 10 KΩ, R6 = R7 = 560 KΩ. The output is also ratiometric to the supply voltage. Shifts in supply voltage will cause shifts in output. The force sensor supply voltage must not to exceed 12 volts (we chose +5V*)*.

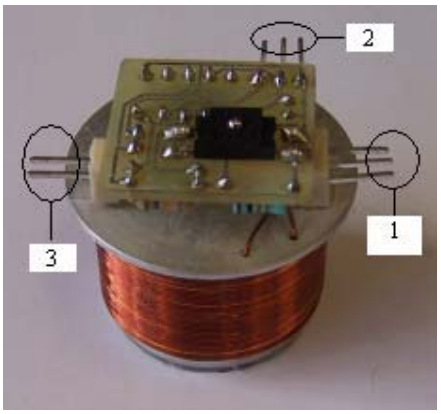

Figure 3-5 Sensor circuit board mounted on the top of aluminium bobbin

The force sensor circuit board is fixed to the top of the aluminium bobbin *(Fig 3.5)*. Port 1 is the solenoid's power supply port; Port 2 provides the power supply to the sensor circuit; Port 3 outputs the feedback force signal to computer.

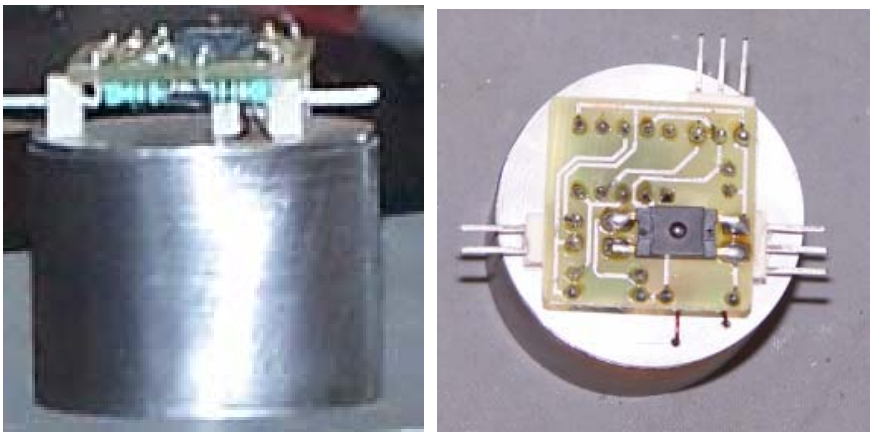

Figure 3-6 Solenoid with sensor circuit board

Fig 3.6 shows the whole solenoid with the sensor circuit board. The sensor's output is in the mV range. This is amplified by the op amp circuit to give a signal in the volts range. This is then output to the computer.

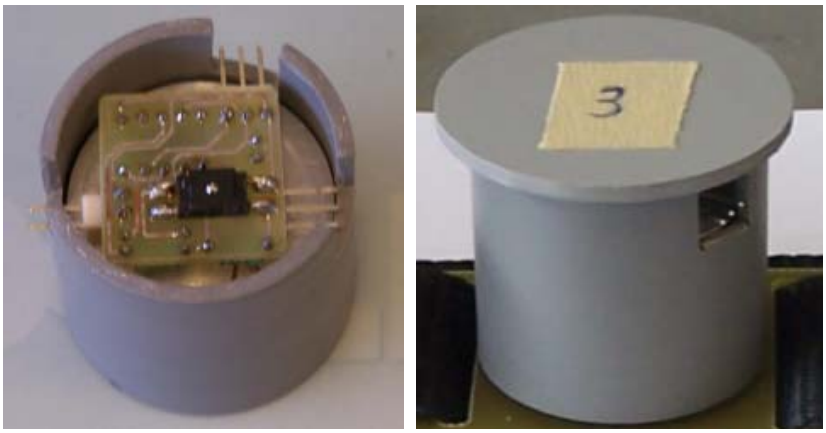

Figure 3-7 Solenoid with PVC shell

The stainless steel ball is very small and the abdomen is flexible. We may get inaccurate results if let the sensor touches the abdomen directly. In order to ensure the accuracy of the results, we made a PVC shell to go around the solenoid. When

the solenoid system is running, the sensor will be pressed by the top part of PVC shell. This will allow a better measurement of the force to be obtained because the PVC is relatively rigid material.

4 SYSTEM TESTING

4.1 Actual force testing of solenoid

The data shown in *Fig 1.8* was just that provided by a model, not the real situation. In order to know the actual force response we can get from the solenoid system, we need to do real world testing. As the *Fig 4.1* shows, the real force is slightly smaller than that predicted by the simulation. But the force curves are similar to those in the simulation and the real generated force is still adequate for our needs. You can see in the following figure, when we input 2 A of current into the coil, the solenoid system produced a force over 14 N.

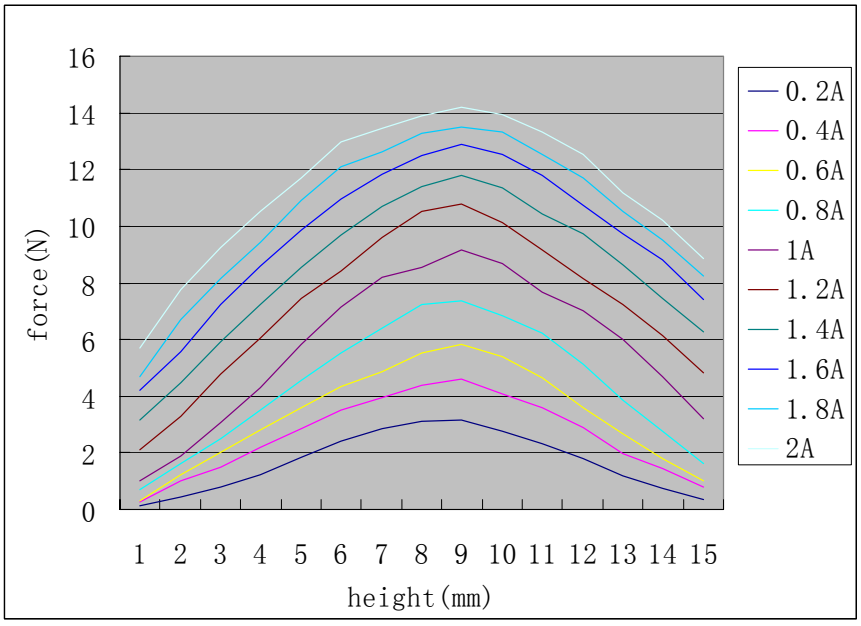

Figure 4-1 Actual force of solenoid schematic diagram

4.2 Testing of solenoid system

The solenoid belt is worn in the manner shown in *Fig2.2*. The belt is tightened using a simple strap length adjuster. It needs to be tight enough so that the

patient's breathing can actually be controlled but not so tight as to cause them undue discomfort when the solenoids extend. This may be highly variable depending on the build of the patient.

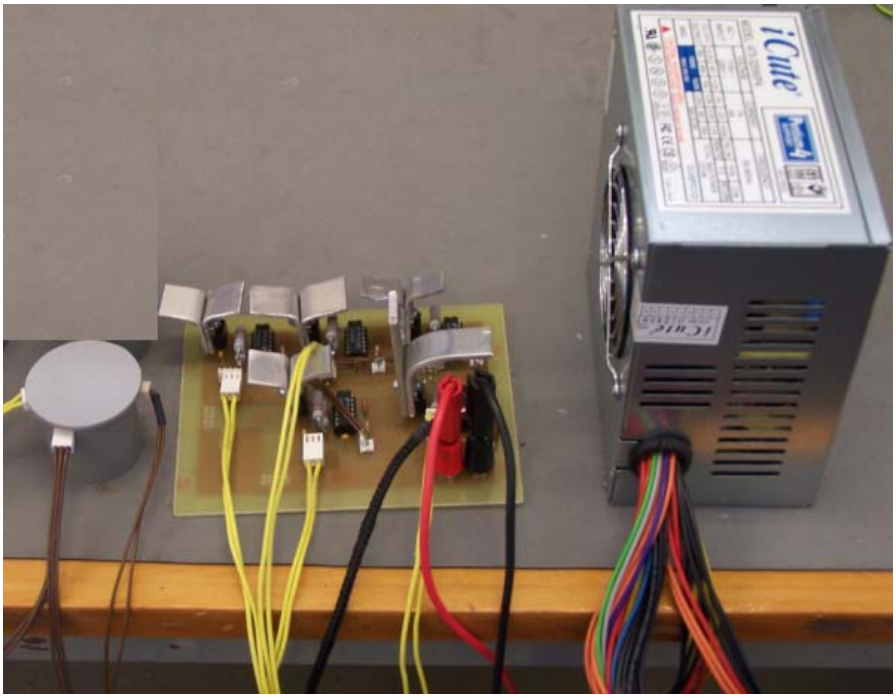

Figure 4-2 View of the system for testing

Fig 4.2 shows the wiring of the system, the yellow wires provide the driving signal to the solenoids. The brown wires coming out of the front of the solenoid provide the power for the force measurement circuitry; these voltages are provided by the power supply on the right hand side. The final wires protruding from the solenoid are the force sensor outputs to be used as the feedback data. And lastly the power from the driver circuit is also provided by a computer power supply.

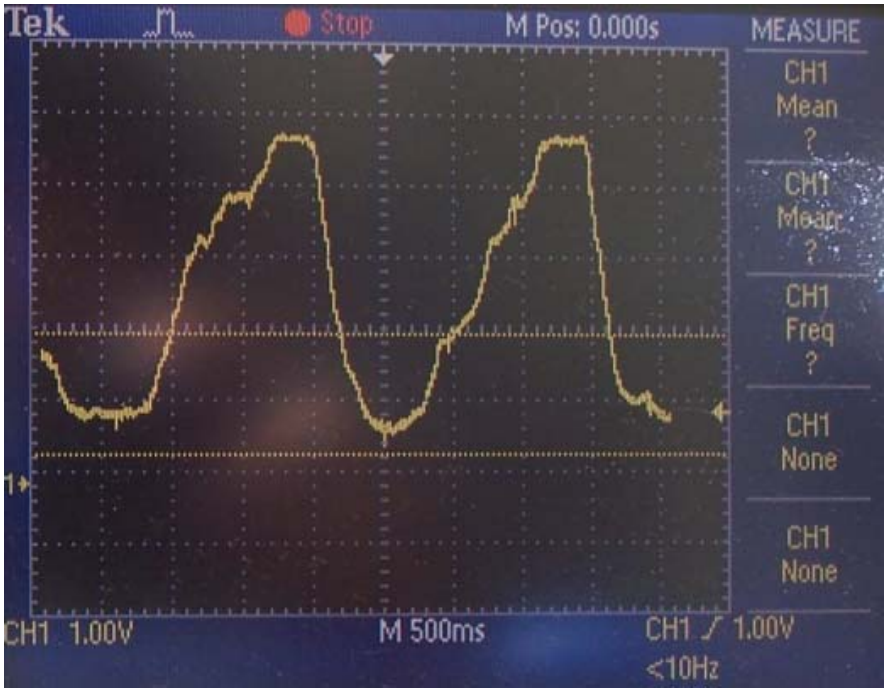

Figure 4-3 Feedback data

Typical force data when the solenoid system is activated is shown in *Fig 4.3*. The range is between 0.4 V and 4.6 V which means 0.15 N to 14.2 N applied to the abdomen. Based on the feedback signal provided by force sensor, the computer can adjust the applied force. The solenoid system performs as expected.

5 FURTHER WORK

Due to the time limit, I have not completed the whole Breathing Stabilization System. A full feedback control system needs to be implemented.

Further developments that will make the system more user–friendly and properly controlled are:

i. Provide a bi – direction drive system so that the solenoid can be actively retracted rather than being pushed back by the patient's abdomen.
ii. Interface the system to a PC.
iii. Ddevelop suitable control algorithms.
iv. Implement a better user interface using Labview.

REFERENCES

[1] Dawson, LA & Sharpe, MB, Image-guided radiotherapy: rationale, benefits, and limitations, Volume 7, Issue 10 Lancet Oncol, 2006, pp. 848-858.

[2] http://en.wikipedia.org/wiki/Image-guided_radiation_therapy.

[3] V. Kini, Patient training in respiratory-gated radiotherapy. Medical Dosimetry , Volume 28 , Issue 1, 2003, pp.7-11.

APPENDIX I SIMULATION OF THE SOLENOID SYSTEM

Modeling Procedure:

For all models, the modeling procedure is very similar:

- ✓ *Define the problem*
- ✓ *Estimate the answer*
- ✓ *Define the modeling method*
- ✓ *Construct the geometry*
- ✓ *Specify the boundary conditions*
- ✓ *Apply the mesh*
- ✓ *Run the solver*
- ✓ *Process the output*

Generally speaking, the early steps are the most important and the most difficult to get right. If you make a mistake running the solver, it is relatively easy to correct. But if you select the wrong method, or worse still, define your problem badly, you could waste days or weeks of effort. (I have wasted a couple of weeks in our project.)

Defining the problem is the most important part of the methodology and is arguably the most difficult. Take time to define it specifically.

Estimating the answer is a valuable step that is so often missed – out in a modeler's rush to get an answer. Use mathematics and physics knowledge to estimate what you would expect the solution to look like. Make some approximations to get the problem tractable on paper if you can. Draw from previous experience. (Whenever I reviewed a piece of modeling work that I had done, I always checked the results against what I expected and queried the results if there was a discrepancy.)

Based on the mathematical model I have established. And the dependent variable in this application mode is the azimuthal component of magnetic vector potential, $\vec{A}_\varphi$ **,** which obeys the relation:

$$(j\omega\sigma - \omega^2\varepsilon)\vec{A}_\varphi + \vec{\nabla}\times(\vec{\mu}^{-1}\vec{\nabla}\times\vec{A}_\varphi) = \vec{J}_\varphi^e \qquad \textit{(Eq. AI.0.1)}$$

where ω is the angular frequency, σ is the electrical conductivity, μ is the permeability, ε is the permittivity, and $\vec{J}_\varphi^e$ denotes the current density due to an external source. One way to define the current source is to specify a distributed current density in the right-hand side of the above equation. This current density gives rise to a current *I* as defined by:

$$\int_s \vec{J}^e \cdot d\vec{s} = I \qquad \textit{(Eq. AI.0.2)}$$

The next step is defining the method. As for our project, we need to know the exactly force when the current go through the coil. Begin a new COMSOL Multiphysics session by invoking the **Model Navigator**. On the **New** tab, select **Axial symmetry 2D** in the **Space dimension** list.In the list of application modes,

click on **Electromagnetics Module**, then select **Quasi-statics, Magnetic>Azimuthal Induction Currents, Vector Potential** and finally **Time-harmonic analysis**. Click **OK** to close the **Model Navigator**.

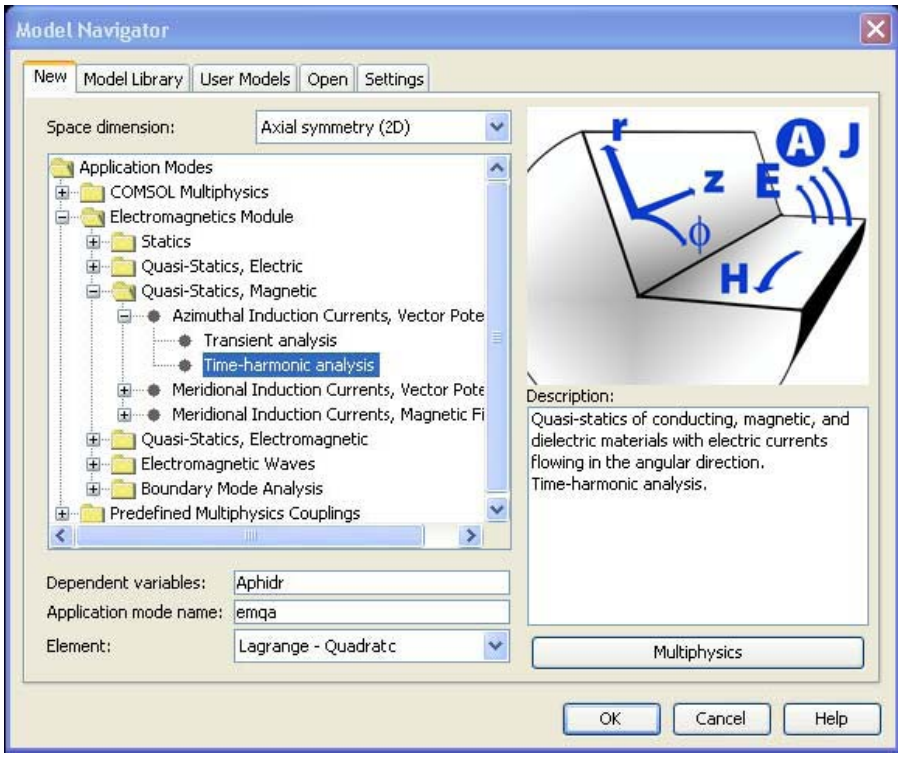

Figure AI-1 Model Navigator

Constructing the geometry is where we define, on the computer, the various shapes and structures that I will use in the modeling. I deconstruct the complex object into smaller, simple object. Because we just need to construct a part description of the object. I can use 2D instead of 3D that will be much easier. Start the modeling session by adjusting the main drawing area to hold the geometry that plan to draw.

i. Select **Axes/Grid Settings** from the **Options** menu to open the **Axes/Grid**

Settings dialog box.

ii. On the **Axis** tab, type -0.05 and 0.5 in the **r min** and **r max** edit fields. Then set the *z* axis limits to -0.3 and 0.3.

iii. To manually define new grid settings, first click the **Grid** tab and then clear the **Auto** check box. Type 0.05 in the **r spacing** edit field and type the value 0.03 in the **Extra r** edit field. Set the value in the **z spacing** edit field to 0.05 and add two extra grid lines by typing -0.01, 0.01 in the **Extra z** edit field.

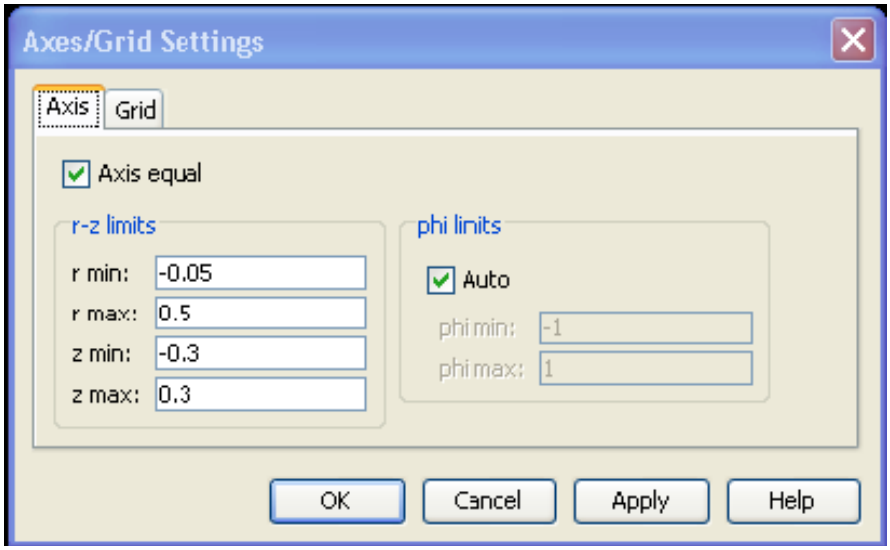

Figure AI-2 Axes/Grid Settings

iv. Click **Apply** to see the effects of the new settings. Notice that the interface adjusts the *r* axis settings to maintain the correct aspect ratio.

v. After that I have drew the follow picture that could describe the situation of whole solenoid.

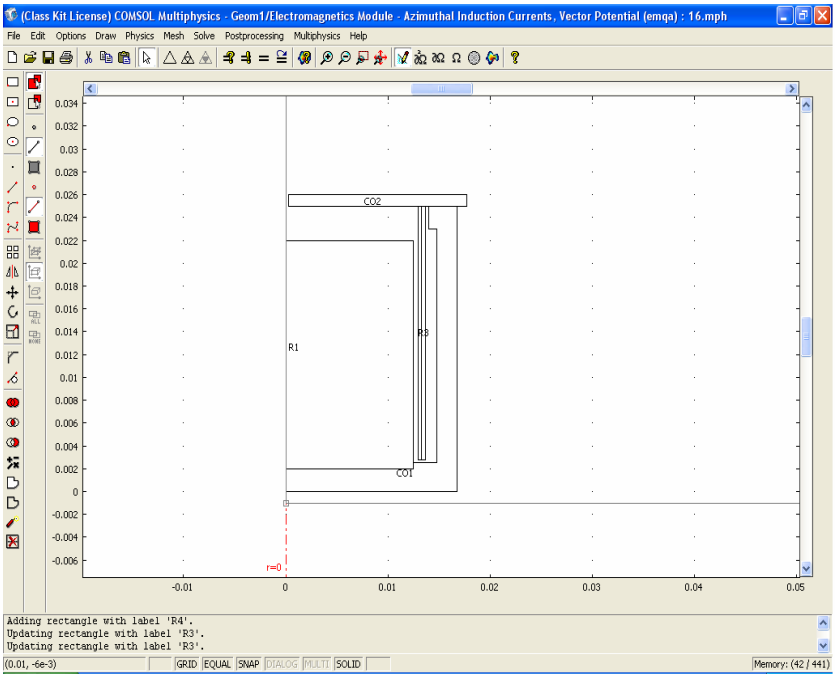

Figure AI-3 Half cross-section of solenoid (a)

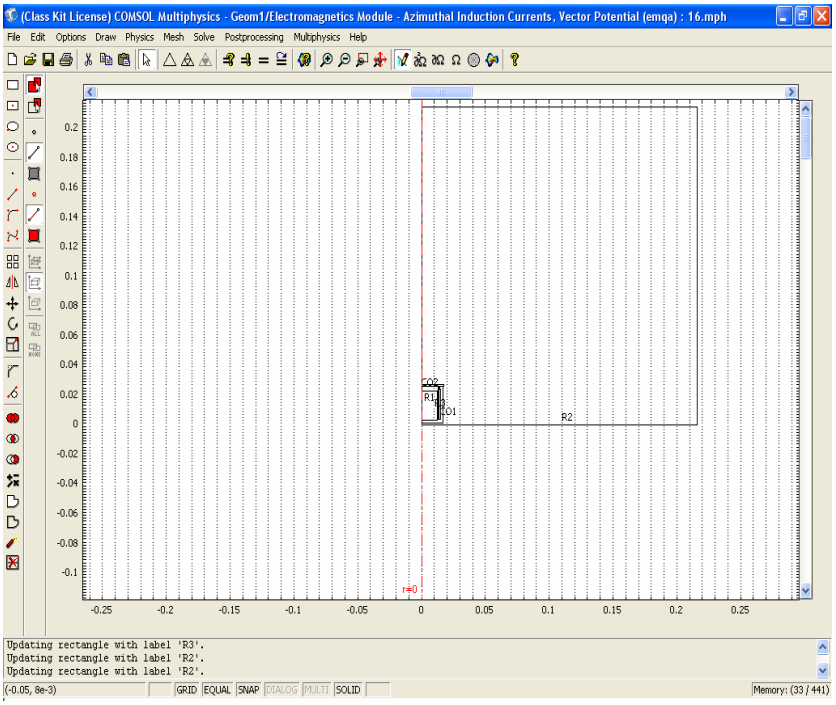

Figure AI-4 Half cross-section of solenoid (b)

BOUNDARY CONDITIONS

i. Open the **Boundary Settings** dialog box by selecting **Boundary Settings**

from the **Physics** menu.

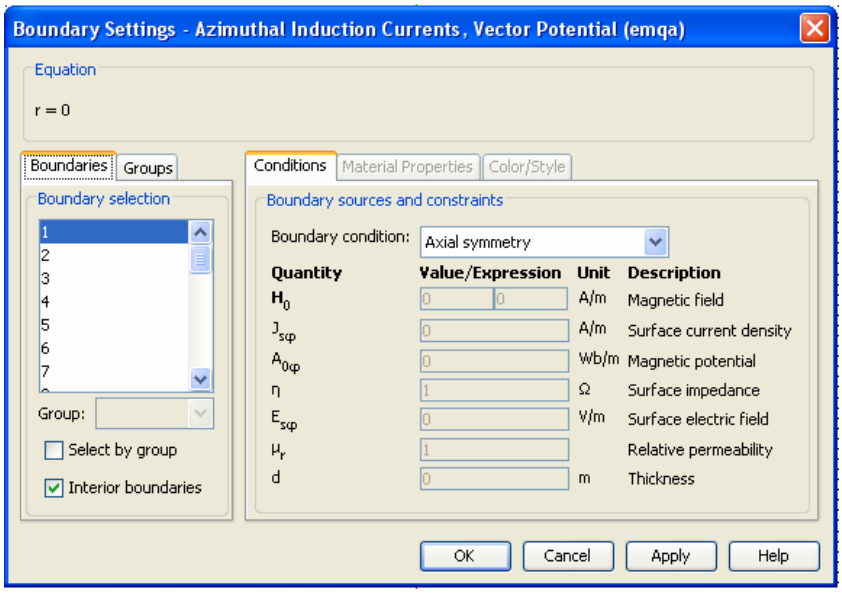

Figure AI-5 Boundary Settings

ii. Enter the boundary conditions according to the following table:

Boundary	**1, 3, 5, 7**	**2, 9, 31**	**4, 6, 8, 10, 11, 12, 13, 14, 15, 16, 17, 18, 19, 20, 21, 22, 23, 24, 25, 26, 27, 28, 29, 30**
Boundary condition	**Axial symmetry**	**Magnetic insulation**	**Continuity**

Table AI-1 Boundary conditions

iii. Click **OK**

Boundaries 1, 3, 5, 7 make up the vertical boundary along the *z* axis, and the axial symmetry boundary condition makes certain the solution is symmetric around this axis. The boundary condition at the other three boundaries (2, 9 and 31) sets the

magnetic potential $\bar{A}_\varphi$ to zero along that boundary. All other boundaries are continuity.

SUBDOMAIN SETTINGS

Select **Subdomain Settings** in the **Physics** menu.

Magnet Parameters:

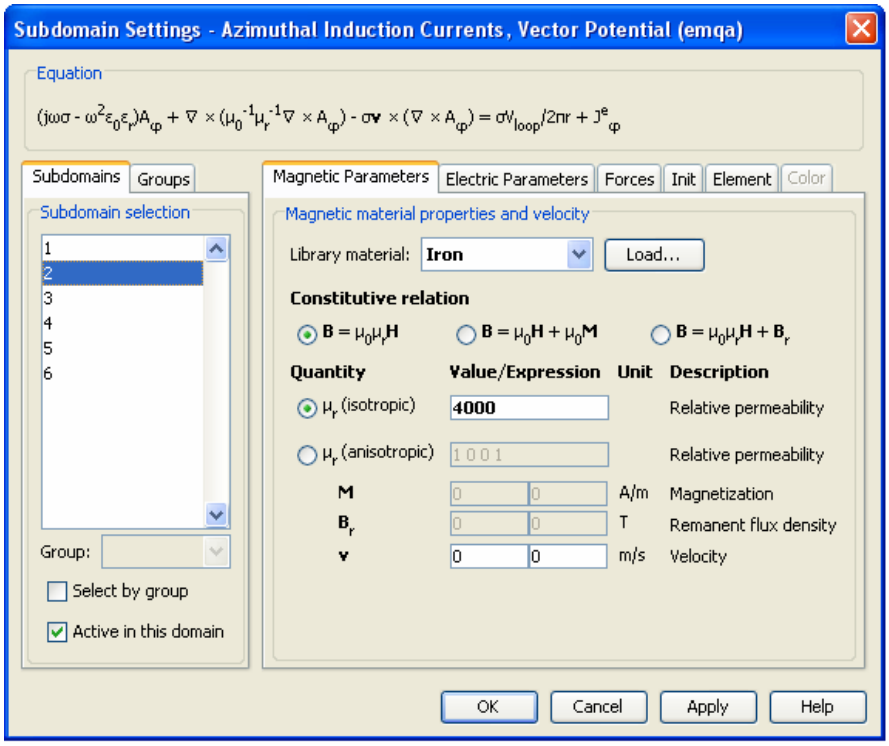

Figure AI-6 Subdomain Settings - magnetic parameters

The Magnetic Parameters for this model appear in the following table. Use default values for any properties not supplied.

Magnetic Parameters	***2***	***3***
μ_r	***4000***	***1.37***
B_r	***0***	***1.2***

Table AI-2 Magnetic Parameters

Electric Parameters:

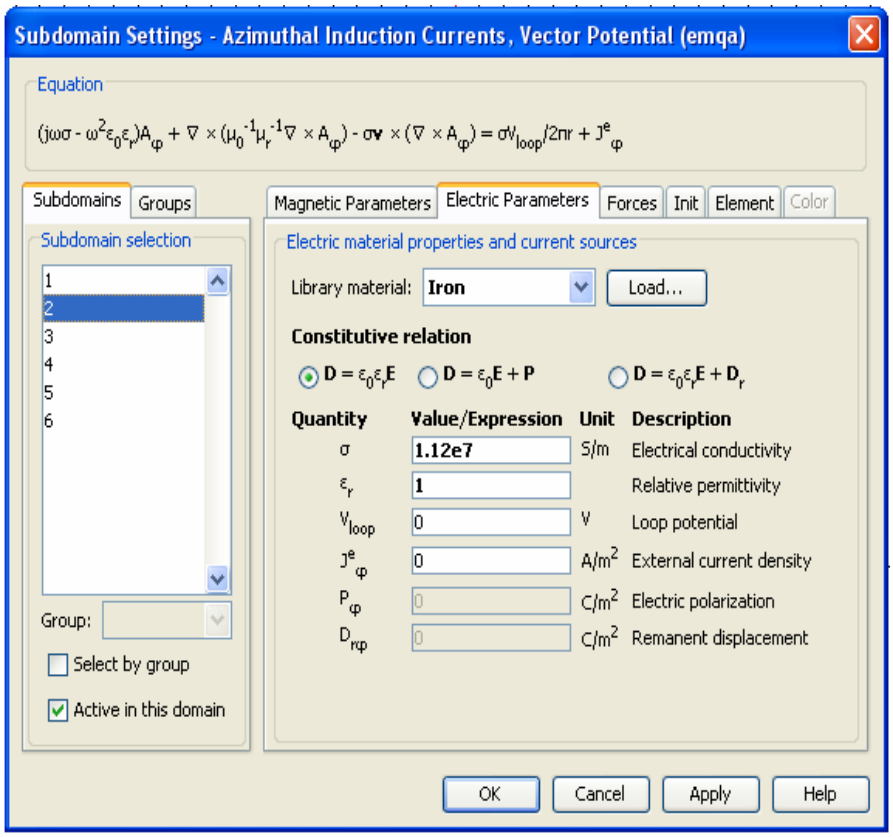

Figure AI-7 Subdomain Settings – electric parameters

The Electric Parameters for this model appear in the following table. Use default values for any properties not supplied.

Electric Parameters	***2, 3***	***4, 5***	***6***
σ	***1.12e7***	***3.774e7***	***5.998e7***
J_{φ}^{e}	***0***	***0***	***-0.81e7***

$(J_{\varphi}^{e} = \frac{I}{A},\ A = \pi\ r^{2})$

Table AI-3 Electric Parameters

MESH GENERATION

In this model, as in many others dealing with electromagnetic phenomena, the effects on fields near the interfaces between materials are of special interest. To get accurate results make sure to generate a very fine mesh in these areas. To do so in this case, refine the mesh one time.

i. To generate a mesh, select **Initialize Mesh** in the **Mesh** menu, or use the corresponding button on the Main toolbar above the main axes area.

ii. Choose **Refine Mesh** in the **Mesh** menu or use the corresponding button on the Main toolbar.

iii. To better see the mesh in the region of interest, choose **Zoom Window** from the **Options** menu. You can now draw a rectangular window around the coil

and the cylinder to get a better view.

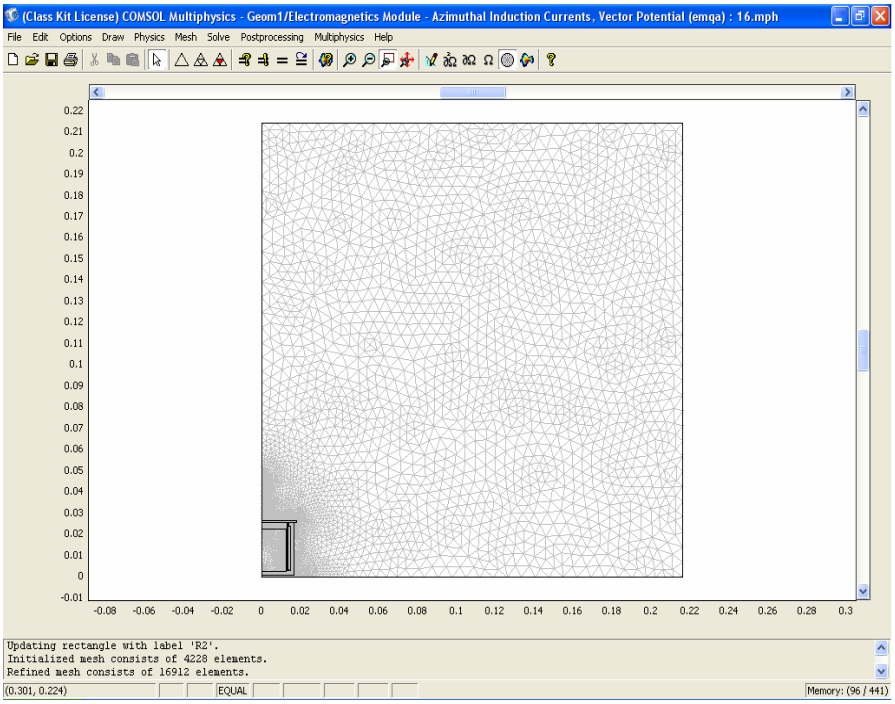

Figure AI-8 Mesh result

COMPUTING THE SOLUTION

Select **Solve Problem** from the **Solve** menu.

POSTPROCESSING AND VISUALIZATION

After solving the problem, the software automatically displays a surface plot for the dependent variable, in this case, the magnetic vector potential. The buttons on the Plot toolbar allow you to generate other types of plots.

To change the default plot parameters follow this procedure:

i. Open up the **Plot Parameters** dialog box by selecting **Plot Parameters** from the **Postprocessing** menu.

ii. On the **General** tab, select the **Surface** and **Streamline** check boxes in the **Plot type** area.

iii. Click the **Surface** tab.

iv. In the **Surface data** area, select **Magnetic flux density, norm** in the **Predefined quantities** list.

v. Click the **Streamline** tab.

vi. Select **Magnetic flux density** from the **Predefined quantities**.

vii. Click **OK** to generate the plot.

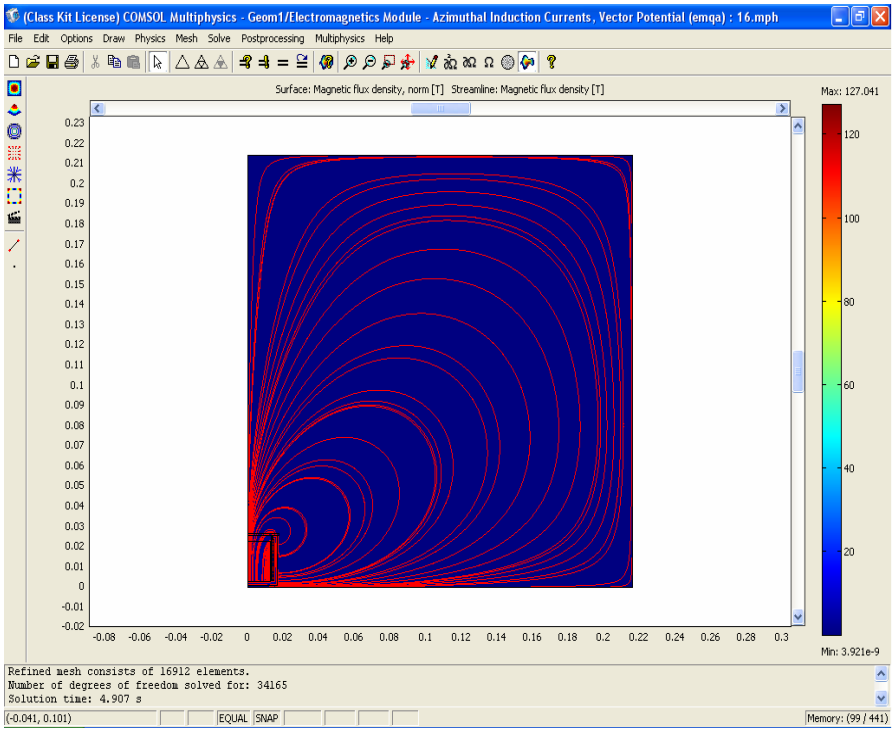

Figure AI-9 Plot result

FORCE CALCULATIONS

To calculate electromagnetic forces in COMSOL using Maxwell's stress tensor

are available in the application mode for quasi-statics. In electrostatics the force is calculated by integrating

$$n_1 T_2 = -\frac{1}{2}\vec{E}\cdot\vec{D} + (\vec{n}_1\cdot\vec{E})\vec{D}^T \qquad \textit{(Eq. AI.3)}$$

On the surface of the object which the force acts on. In magnet-statics and quasi-statics the expression

$$n_1 T_2 = -\frac{1}{2}\vec{H}\cdot\vec{B} + (\vec{n}_1\cdot\vec{H})\vec{B}^T \qquad \textit{(Eq. AI.4)}$$

is integrated on the surface to obtain the force. $\vec{E}$ is the electric field, $\vec{D}$ the electric displacement, $\vec{H}$ the magnetic field, $\vec{B}$ the magnetic flux density, and $\vec{n}_1$ the outward normal from the object.

DEFINING FORCE VARIABLES

Define force variables in the **Subdomain Settings** dialog box. On the **Forces** tab there is a table where you define the variables. Select the two subdomains representing the iron and enter a name a.

This generates a set of variables. There are two variables a_nTr_emqa and a_nTz_emqa defined on the exterior boundary of the solenoid. These are Maxwell stress tensor on the surface in the *r* and *z* directions and represent a surface force density. Two scalar variables, a_forcer_emqa and a_forcez_emqa, are also generated, which are the total force on the solenoid in the *r* and *z* directions.

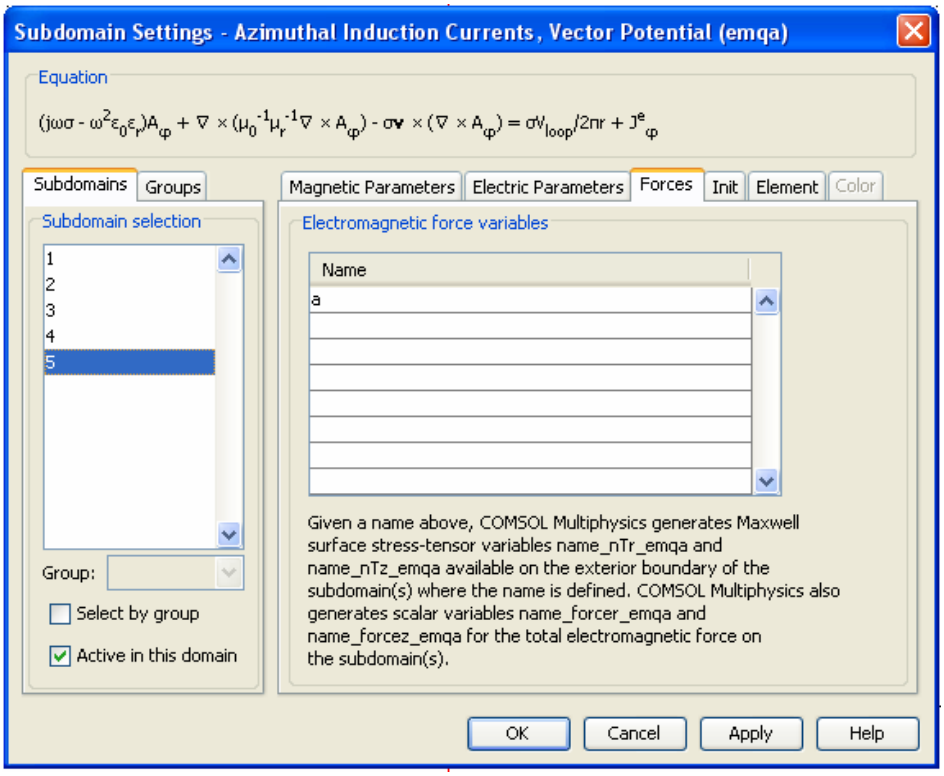

Figure AI-10 Subdomain Settings – force parameters

RESULTS

To display the forces on the solenoid you can use the **Data Display** dialog box. Enter the expression a_forcez_emqa and click **OK** to obtain the force in the *z* direction. Because the variable a_forcez_emqa is a scalar it is possible to evaluate it in any point. That's what we want to know.

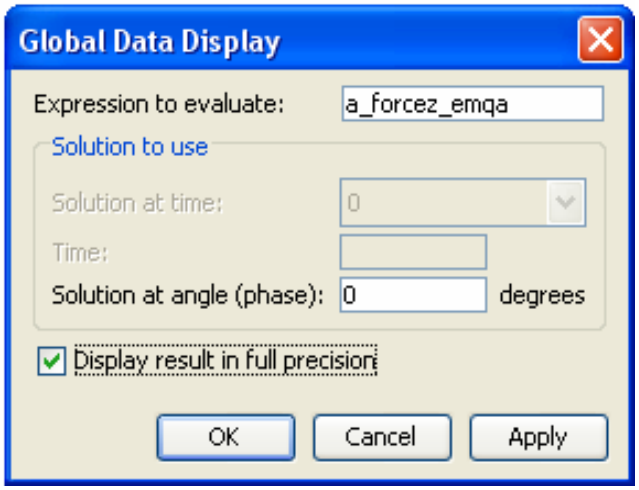

Figure AI-11 Data display

APPENDIX II DATASHEETS

- ✓ **Datasheet of force sensor FSS1500NST**
- ✓ **Datasheet of J-FET operational amplifier TL081**
- ✓ **Datasheet of low power quad operational amplifier LM324**

Honeywell

Force Sensors

FSS Low Profile Force Sensors

FS Series

FEATURES

- True Surface Mount Technology
- Maximum peak reflow temperature of 260 °C [500 °F]
- Compact, commercial grade package
- Robust performance characteristics
- Adaptable package design
- Precision force sensing
- Reliability rated at 20 million MCTF at 25 °C [77 °F]
- Electrically ratiometric output
- Extremely low deflection (30 microns typ. @ Full Scale)
- High ESD resistance 8 kV
- Available signal conditioning
- Optional terminal configurations

TYPICAL APPLICATIONS

- Medical infusion pumps
- Ambulatory noninvasive pump pressure
- Occlusion detection
- Kidney dialysis machines
- Load and compression sensing
- Variable tensions control
- Robotic end-effectors
- Wire bonding equipment

⚠ WARNING

PERSONAL INJURY

DO NOT USE these products as safety or emergency stop devices or in any other application where failure of the product could result in personal injury.

Failure to comply with these instructions could result in death or serious injury.

The FS Series sensors provide precise reliable force sensing performance in a compact commercial grade package at a cost effective price. The sensor features a proven sensing technology that uses a specialized piezoresistive micromachined silicon sensing element. The low power, unamplified, uncompensated Wheatstone bridge circuit design provides inherently stable mV outputs over the force range.

Force sensors operate on the principle that the resistance of silicon-implanted piezoresistors will increase when the resistors flex under any applied force. The sensor concentrates force from the applications, through the stainless steel ball, directly to the silicon-sensing element. The amount of resistance changes in proportion to the amount of force being applied. This change in circuit resistance results in a corresponding mV output level change.

The sensor package design incorporates patented modular construction. The use of innovative elastomeric technology and engineered molded plastics result in load excitation capacities of 4.5/5.5 kg over-force. The stainless steel ball provides excellent mechanical stability and is adaptable to a variety of applications. The FSS sensor delivered 20 million operations in Mean Cycles to Failure (MCTF) reliability testing at 50 °C [122 °F]. This test determines the number of possible sensor operations at full scale until failure. Various electric interconnects can accept prewired connectors, printed circuit board mounting, and surface mountings. The unique sensor design also provides a variety of mounting options that include mounting brackets, as well as application specific mounting requirements.

⚠ WARNING

MISUSE OF DOCUMENTATION

- The information presented in this product sheet is for reference only. Do not use this document as a product installation guide.
- Complete installation, operation, and maintenance information is provided in the instructions supplied with each product.

Failure to comply with these instructions could result in death or serious injury.

PERFORMANCE CHARACTERISTICS @ 5.0 ± 0.01 Vdc Excitation*, 25 °C [77 °F]

Parameter	Min.	Typical	Max.	Units
Null Offset	-15	0	+15	mV
Operating Force	0	–	1500	grams
Sensitivity.	0.1	0.12	14	mV/gram
Linearity (B.FS.L.)**	–	± 1.5	–	% span
Repeatability @ 300 g	–	± 10	–	grams
Null Shift				
25 °C to 2 °C [77 °F to 35.6 °F]	–	± 0.5	–	mV
25 °C to 40 °C [77 °F to 104 °F]	–	± 0.5	–	mV
Sensitivity Shift				
25 °C to 50 °C [77 °F to 122 °F]	–	5.5	–	% span
25 °C to 0 °C [77 °F to 32 °F]	–	5.5	–	% span
Input Resistance	4.0 K	5.0 K	6.0 K	Ohms
Output Resistance	4.0 K	5.0 K	6.0 K	Ohms
Overforce	–	–	4,500	grams
ESD (direct contact, terminals and plunger)	8	–	–	kV

* Non-compensated force sensors, excited by constant current (1.5 mA) instead of voltage, exhibit partial temperature compensation of Span.

** BFSL: Best Fit Straight Line

ENVIRONMENTAL SPECIFICATIONS

Operating temperature	-40 °C to 85 °C [-40 °F to 185 °F]
Storage temperature	-40 °C to 100 °C [-40°F to 212 °F]
Shock	Qualification tested to 150 g
Vibration	Qualification tested to 0 to 2 kHz, 20 g sine
MCTF	20 million at 25 °C [77 °F]
Solderability	5 sec at 315 °C [599 °F] per lead
Output ratiometric	Within supply range

Note: All force related specifications are established using dead weight or compliant force.

SENSOR PINOUT

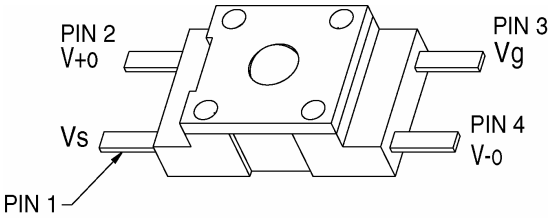

EXCITATION SCHEMATIC
Excitation 5 Vdc Typ., 12 Vdc Max.

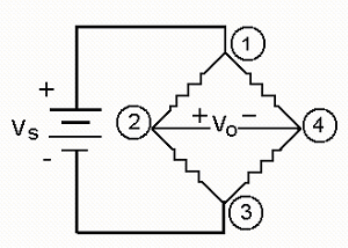

FS SERIES CIRCUIT

1. Circled numbers refer to sensor terminals (pins).
   Pin 1 = Supply V_S (+)
   Pin 2 = Output Vo (+)
   Pin 3 = Ground V_g (-)
   Pin 4 = Output V_O (-)
2. The force sensor may be powered by voltage or current. Maximum supply voltage is not to exceed 12 volts. Maximum supply current is not to exceed 1.6 mA. Power is applied across Pin 1 and Pin 3.
3. The sensor output should be measured as a differential voltage across Pin 2 and Pin 4 ($V_O = V_2 - V_4$). The output is ratiometric to the supply voltage. Shifts in supply voltage will cause shifts in output. Neither Pin 2 nor Pin 4 should be tied to ground or voltage supply.

MOUNTING DIMENSIONS (for reference only) mm/in

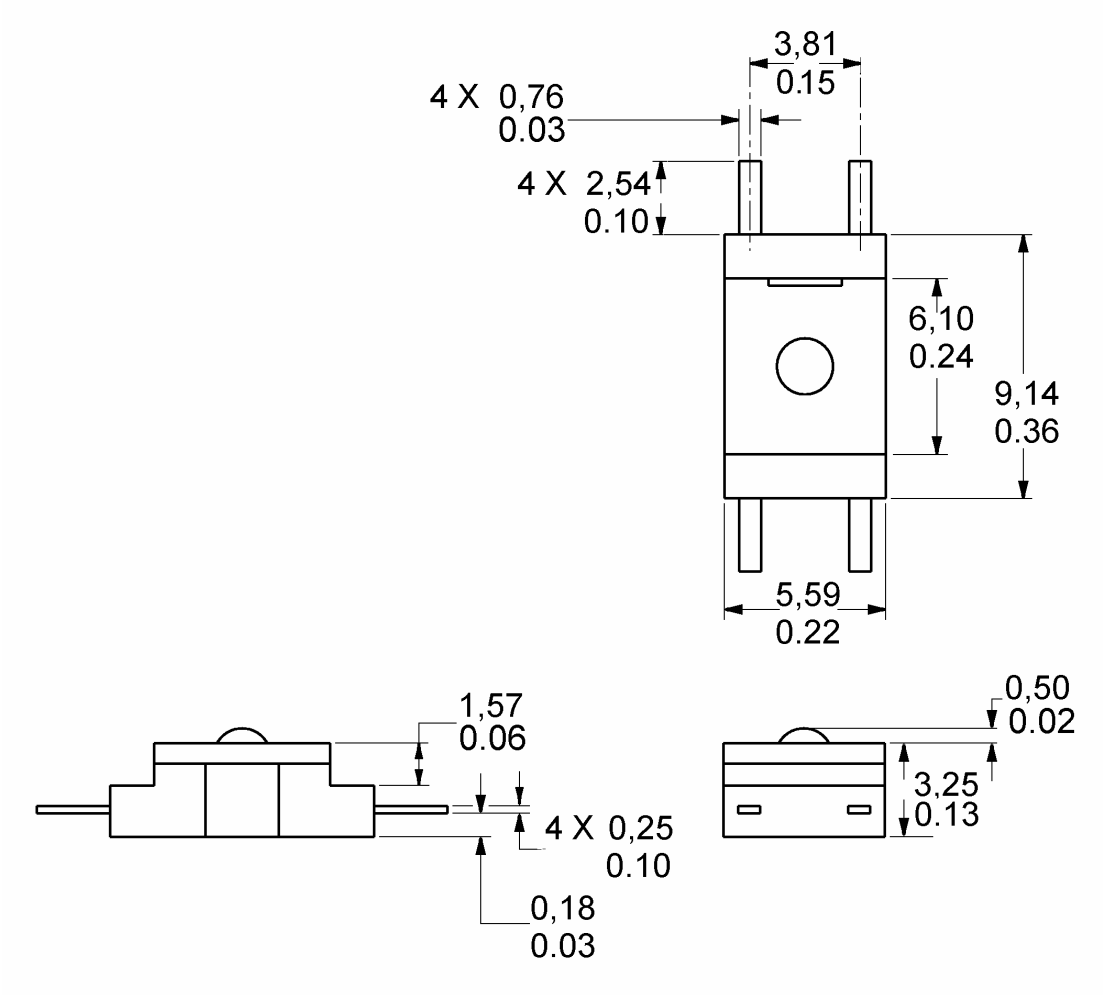

DESCRIPTION

Catalog Listing	Packing Style
FSS1500NST	Tube
FSS1500NSB	Bubble Pack
FSS1500NSR	Tape and Reel

WARRANTY/REMEDY
Honeywell warrants goods of its manufacture as being free of defective materials and faulty workmanship. Contact your local sales office for warranty information. If warranted goods are returned to Honeywell during the period of coverage, Honeywell will repair or replace without charge those items it finds defective. **The foregoing is Buyer's sole remedy and is in lieu of all other warranties, expressed or implied, including those of merchantability and fitness for a particular purpose.**
Specifications may change without notice. The information we supply is believed to be accurate and reliable as of this printing. However, we assume no responsibility for its use.

While we provide application assistance personally, through our literature and the Honeywell web site, it is up to the customer to determine the suitability of the product in the application.
For application assistance, current specifications, or name of the nearest Authorized Distributor, contact a nearby sales office. Or call:
1-800-537-6945 USA
1-800-737-3360 Canada
1-815-235-6847 International
FAX
1-815-235-6545 USA
INTERNET
www.honeywell.com/sensing
info.sc@honeywell.com

Honeywell

Sensing and Control
Honeywell
11 West Spring Street
Freeport, Illinois 61032
0080809-1-EN IL50 GLO 803 Printed in USA

TL081
TL081A - TL081B

GENERAL PURPOSE J-FET SINGLE OPERATIONAL AMPLIFIER

- WIDE COMMON-MODE (UP TO V_{CC}^+) AND DIFFERENTIAL VOLTAGE RANGE
- LOW INPUT BIAS AND OFFSET CURRENT
- OUTPUT SHORT-CIRCUIT PROTECTION
- HIGH INPUT IMPEDANCE J–FET INPUT STAGE
- INTERNAL FREQUENCY COMPENSATION
- LATCH UP FREE OPERATION
- HIGH SLEW RATE : 16V/µs (typ)

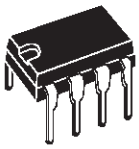

N
DIP8
(Plastic Package)

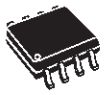

D
SO8
(Plastic Micropackage)

DESCRIPTION

The TL081, TL081A and TL081B are high speed J–FET input single operational amplifiers incorporating well matched, high voltage J–FET and bipolar transistors in a monolithic integrated circuit.

The devices feature high slew rates, low input bias and offset currents, and low offset voltage temperature coefficient.

ORDER CODES

Part Number	Temperature Range	Package	
		N	D
TL081M/AM/BM	–55°C, +125°C	•	•
TL081I/AI/BI	–40°C, +105°C	•	•
TL081C/AC/BC	0°C, +70°C	•	•
Examples : TL081CD, TL081IN			

PIN CONNECTIONS (top view)

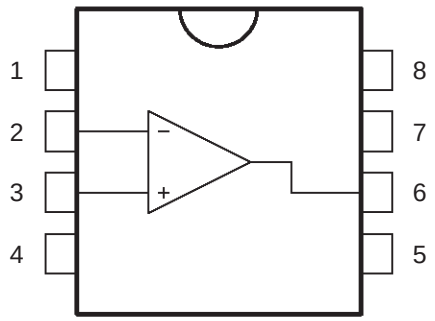

1 - Offset Null 1
2 - Inverting input
3 - Non-inverting input
4 - V_{CC}^-
5 - Offset Null 2
6 - Output
7 - V_{CC}^+
8 - N.C.

SCHEMATIC DIAGRAM

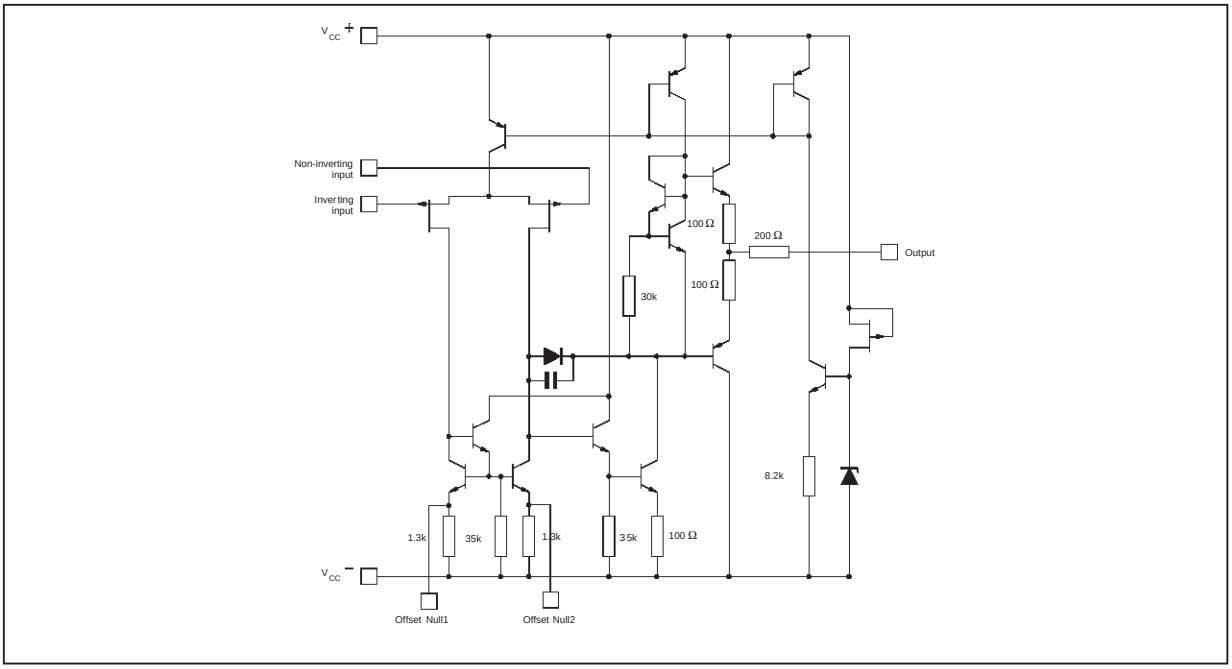

INPUT OFFSET VOLTAGE NULL CIRCUITS

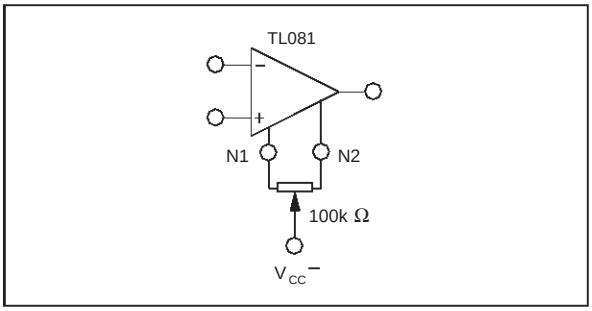

ABSOLUTE MAXIMUM RATINGS

Symbol	Parameter		Value	Unit
V_{CC}	Supply Voltage - (note 1)		±18	V
V_i	Input Voltage - (note 3)		±15	V
V_{id}	Differential Input Voltage - (note 2)		±30	V
P_{tot}	Power Dissipation		680	mW
	Output Short-circuit Duration - (note 4)		Infinite	
T_{oper}	Operating Free Air Temperature Range	TL081C,AC,BC TL081I,AI,BI TL081M,AM,BM	0 to 70 –40 to 105 –55 to 125	°C
T_{stg}	Storage Temperature Range		–65 to 150	°C

Notes :
1. All voltage values, except differential voltage, are with respect to the zero reference level (ground) of the supply voltages where the zero reference level is the midpoint between V_{CC}^+ and V_{CC}^-.
2. Differential voltages are at the non-inverting input terminal with respect to the inverting input terminal.
3. The magnitude of the input voltage must never exceed the magnitude of the supply voltage or 15 volts, whichever is less.
4. The output may be shorted to ground or to either supply. Temperature and /or supply voltages must be limited to ensure that the dissipation rating is not exceeded.

ELECTRICAL CHARACTERISTICS

V_{CC} = ±15V, T_{amb} = 25°C (unless otherwise specified)

Symbol	Parameter		TL081I,M,AC,AI, AM,BC,BI,BM			TL081C			Unit
			Min.	Typ.	Max.	Min.	Typ.	Max.	
V_{io}	Input Offset Voltage (R_S = 50Ω) T_{amb} = 25°C $T_{min.} \le T_{amb} \le T_{max.}$	TL081 TL081A TL081B TL081 TL081A TL081B		3 3 1	10 6 3 13 7 5		3	10 13	mV
DV_{io}	Input Offset Voltage Drift			10			10		µV/°C
I_{io}	Input Offset Current * T_{amb} = 25°C $T_{min.} \le T_{amb} \le T_{max.}$			5	100 4		5	100 4	pA nA
I_{ib}	Input Bias Current * T_{amb} = 25°C $T_{min.} \le T_{amb} \le T_{max.}$			20	200 20		20	400 20	pA nA
A_{vd}	Large Signal Voltage Gain (R_L = 2kΩ, V_O = ±10V) T_{amb} = 25°C $T_{min.} \le T_{amb} \le T_{max.}$		50 25	200		25 15	200		V/mV
SVR	Supply Voltage Rejection Ratio (R_S = 50Ω) T_{amb} = 25°C $T_{min.} \le T_{amb} \le T_{max.}$		80 80	86		70 70	86		dB
I_{CC}	Supply Current, no Load T_{amb} = 25°C $T_{min.} \le T_{amb} \le T_{max.}$			1.4	2.5 2.5		1.4	2.5 2.5	mA
V_{icm}	Input Common Mode Voltage Range		±11	+15 -12		±11	+15 -12		V
CMR	Common Mode Rejection Ratio (R_S = 50Ω) T_{amb} = 25°C $T_{min.} \le T_{amb} \le T_{max.}$		80 80	86		70 70	86		dB
Ios	Output Short-circuit Current T_{amb} = 25°C $T_{min.} \le T_{amb} \le T_{max.}$		10 10	40	60 60	10 10	40	60 60	mA
$\pm V_{OPP}$	Output Voltage Swing T_{amb} = 25°C $T_{min.} \le T_{amb} \le T_{max.}$	R_L = 2kΩ R_L = 10kΩ R_L = 2kΩ R_L = 10kΩ	10 12 10 12	12 13.5		10 12 10 12	12 13.5		V
SR	Slew Rate (V_{in} = 10V, R_L = 2kΩ, C_L = 100pF, T_{amb} = 25°C, unity gain)		8	16		8	16		V/µs
t_r	Rise Time (V_{in} = 20mV, R_L = 2kΩ, C_L = 100pF, T_{amb} = 25°C, unity gain)			0.1			0.1		µs
K_{OV}	Overshoot (V_{in} = 20mV, R_L = 2kΩ, C_L = 100pF, T_{amb} = 25°C, unity gain)			10			10		%
GBP	Gain Bandwidth Product (f = 100kHz, T_{amb} = 25°C, V_{in} = 10mV, R_L = 2kΩ, C_L = 100pF)		2.5	4		2.5	4		MHz
R_i	Input Resistance			10^{12}			10^{12}		Ω
THD	Total Harmonic Distortion (f = 1kHz, A_V = 20dB, R_L = 2kΩ, C_L = 100pF, T_{amb} = 25°C, V_O = 2V_{PP})			0.01			0.01		%
e_n	Equivalent Input Noise Voltage (f = 1kHz, R_s = 100Ω)			15			15		$\frac{nV}{\sqrt{Hz}}$
∅m	Phase Margin			45			45		Degrees

* The input bias currents are junction leakage currents which approximately double for every 10°C increase in the junction temperature.

National Semiconductor

August 2000

LM124/LM224/LM324/LM2902
Low Power Quad Operational Amplifiers

General Description

The LM124 series consists of four independent, high gain, internally frequency compensated operational amplifiers which were designed specifically to operate from a single power supply over a wide range of voltages. Operation from split power supplies is also possible and the low power supply current drain is independent of the magnitude of the power supply voltage.

Application areas include transducer amplifiers, DC gain blocks and all the conventional op amp circuits which now can be more easily implemented in single power supply systems. For example, the LM124 series can be directly operated off of the standard +5V power supply voltage which is used in digital systems and will easily provide the required interface electronics without requiring the additional ±15V power supplies.

Unique Characteristics

- In the linear mode the input common-mode voltage range includes ground and the output voltage can also swing to ground, even though operated from only a single power supply voltage
- The unity gain cross frequency is temperature compensated
- The input bias current is also temperature compensated

Advantages

- Eliminates need for dual supplies
- Four internally compensated op amps in a single package
- Allows directly sensing near GND and V_{OUT} also goes to GND
- Compatible with all forms of logic
- Power drain suitable for battery operation

Features

- Internally frequency compensated for unity gain
- Large DC voltage gain 100 dB
- Wide bandwidth (unity gain) 1 MHz (temperature compensated)
- Wide power supply range:
  Single supply 3V to 32V
  or dual supplies ±1.5V to ±16V
- Very low supply current drain (700 µA)—essentially independent of supply voltage
- Low input biasing current 45 nA (temperature compensated)
- Low input offset voltage 2 mV and offset current: 5 nA
- Input common-mode voltage range includes ground
- Differential input voltage range equal to the power supply voltage
- Large output voltage swing 0V to V^+ – 1.5V

Connection Diagrams

Dual-In-Line Package

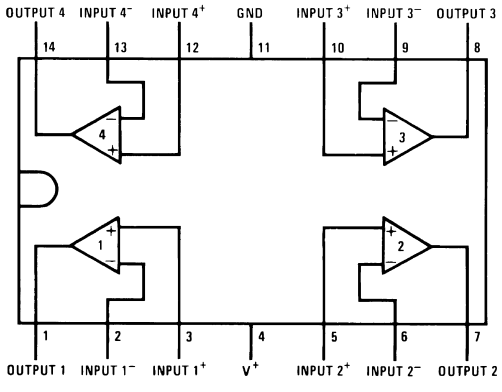

00929901

Top View

Order Number LM124J, LM124AJ, LM124J/883 (Note 2)**, LM124AJ/883** (Note 1)**, LM224J, LM224AJ, LM324J, LM324M, LM324MX, LM324AM, LM324AMX, LM2902M, LM2902MX, LM324N, LM324AN, LM324MT, LM324MTX or LM2902N LM124AJRQML and LM124AJRQMLV**(Note 3)

See NS Package Number J14A, M14A or N14A

Connection Diagrams (Continued)

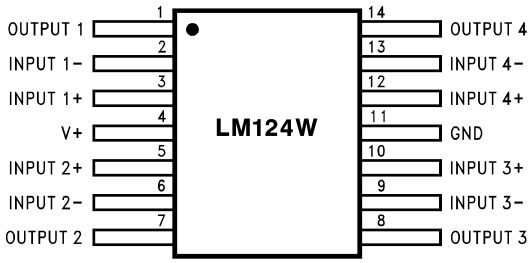

00929933

Order Number LM124AW/883, LM124AWG/883, LM124W/883 or LM124WG/883
LM124AWRQML and LM124AWRQMLV(Note 3)
See NS Package Number W14B
LM124AWGRQML and LM124AWGRQMLV(Note 3)
See NS Package Number WG14A

Note 1: LM124A available per JM38510/11006

Note 2: LM124 available per JM38510/11005

Note 3: See STD Mil DWG 5962R99504 for Radiation Tolerant Device

Schematic Diagram (Each Amplifier)

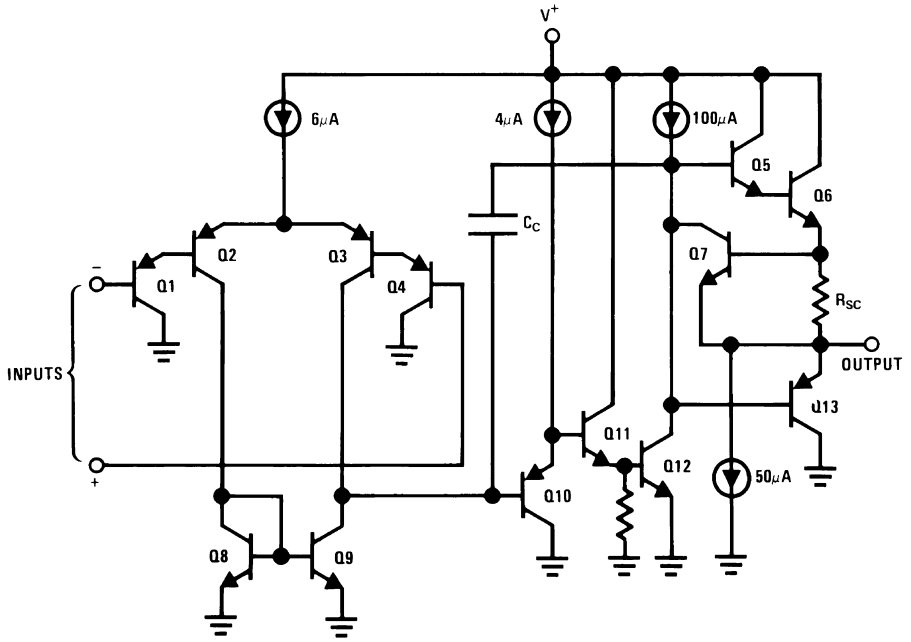

00929902

Absolute Maximum Ratings (Note 12)

If Military/Aerospace specified devices are required, please contact the National Semiconductor Sales Office/ Distributors for availability and specifications.

	LM124/LM224/LM324 LM124A/LM224A/LM324A	LM2902
Supply Voltage, V^+	32V	26V
Differential Input Voltage	32V	26V
Input Voltage	−0.3V to +32V	−0.3V to +26V
Input Current		
(V_{IN} < −0.3V) (Note 6)	50 mA	50 mA
Power Dissipation (Note 4)		
Molded DIP	1130 mW	1130 mW
Cavity DIP	1260 mW	1260 mW
Small Outline Package	800 mW	800 mW
Output Short-Circuit to GND		
(One Amplifier) (Note 5)		
$V^+ \leq 15V$ and $T_A = 25^\circ C$	Continuous	Continuous
Operating Temperature Range		−40˚C to +85˚C
LM324/LM324A	0˚C to +70˚C	
LM224/LM224A	−25˚C to +85˚C	
LM124/LM124A	−55˚C to +125˚C	
Storage Temperature Range	−65˚C to +150˚C	−65˚C to +150˚C
Lead Temperature (Soldering, 10 seconds)	260˚C	260˚C
Soldering Information		
Dual-In-Line Package		
Soldering (10 seconds)	260˚C	260˚C
Small Outline Package		
Vapor Phase (60 seconds)	215˚C	215˚C
Infrared (15 seconds)	220˚C	220˚C
See AN-450 "Surface Mounting Methods and Their Effect on Product Reliability" for other methods of soldering surface mount devices.		
ESD Tolerance (Note 13)	250V	250V

Electrical Characteristics

$V^+ = +5.0V$, (Note 7), unless otherwise stated

Parameter	Conditions	LM124A			LM224A			LM324A			Units
		Min	Typ	Max	Min	Typ	Max	Min	Typ	Max	
Input Offset Voltage	(Note 8) $T_A = 25^\circ C$		1	2		1	3		2	3	mV
Input Bias Current (Note 9)	$I_{IN(+)}$ or $I_{IN(-)}$, $V_{CM} = 0V$, $T_A = 25^\circ C$		20	50		40	80		45	100	nA
Input Offset Current	$I_{IN(+)}$ or $I_{IN(-)}$, $V_{CM} = 0V$, $T_A = 25^\circ C$		2	10		2	15		5	30	nA
Input Common-Mode Voltage Range (Note 10)	$V^+ = 30V$, (LM2902, $V^+ = 26V$), $T_A = 25^\circ C$	0		V^+−1.5	0		V^+−1.5	0		V^+−1.5	V
Supply Current	Over Full Temperature Range $R_L = \infty$ On All Op Amps										mA
	$V^+ = 30V$ (LM2902 $V^+ = 26V$)		1.5	3		1.5	3		1.5	3	
	$V^+ = 5V$		0.7	1.2		0.7	1.2		0.7	1.2	
Large Signal Voltage Gain	$V^+ = 15V$, $R_L \geq 2k\Omega$, ($V_O = 1V$ to 11V), $T_A = 25^\circ C$	50	100		50	100		25	100		V/mV
Common-Mode	DC, $V_{CM} = 0V$ to $V^+ - 1.5V$,	70	85		70	85		65	85		dB

Electrical Characteristics (Continued)

V^+ = +5.0V, (Note 7), unless otherwise stated

Parameter		Conditions		LM124A			LM224A			LM324A			Units
				Min	Typ	Max	Min	Typ	Max	Min	Typ	Max	
Rejection Ratio		T_A = 25˚C											
Power Supply Rejection Ratio		V^+ = 5V to 30V (LM2902, V^+ = 5V to 26V), T_A = 25˚C		65	100		65	100		65	100		dB
Amplifier-to-Amplifier Coupling (Note 11)		f = 1 kHz to 20 kHz, T_A = 25˚C (Input Referred)			−120			−120			−120		dB
Output Current	Source	V_{IN}^+ = 1V, V_{IN}^- = 0V, V^+ = 15V, V_O = 2V, T_A = 25˚C		20	40		20	40		20	40		mA
	Sink	V_{IN}^- = 1V, V_{IN}^+ = 0V, V^+ = 15V, V_O = 2V, T_A = 25˚C		10	20		10	20		10	20		mA
		V_{IN}^- = 1V, V_{IN}^+ = 0V, V^+ = 15V, V_O = 200 mV, T_A = 25˚C		12	50		12	50		12	50		µA
Short Circuit to Ground		(Note 5) V^+ = 15V, T_A = 25˚C			40	60		40	60		40	60	mA
Input Offset Voltage		(Note 8)				4			4			5	mV
V_{OS} Drift		R_S = 0Ω			7	20		7	20		7	30	µV/˚C
Input Offset Current		$I_{IN(+)} - I_{IN(-)}$, V_{CM} = 0V				30			30			75	nA
I_{OS} Drift		R_S = 0Ω			10	200		10	200		10	300	pA/˚C
Input Bias Current		$I_{IN(+)}$ or $I_{IN(-)}$			40	100		40	100		40	200	nA
Input Common-Mode Voltage Range (Note 10)		V^+ = +30V (LM2902, V^+ = 26V)		0		V^+–2	0		V^+–2	0		V^+–2	V
Large Signal Voltage Gain		V^+ = +15V (V_OSwing = 1V to 11V) $R_L \geq 2$ kΩ		25			25			15			V/mV
Output Voltage Swing	V_{OH}	V^+ = 30V	R_L = 2 kΩ	26			26			26			V
		(LM2902, V^+ = 26V)	R_L = 10 kΩ	27	28		27	28		27	28		
	V_{OL}	V^+ = 5V, R_L = 10 kΩ			5	20		5	20		5	20	mV
Output Current	Source	V_O = 2V	V_{IN}^+ = +1V, V_{IN}^- = 0V, V^+ = 15V	10	20		10	20		10	20		mA
	Sink		V_{IN}^- = +1V, V_{IN}^+ = 0V, V^+ = 15V	10	15		5	8		5	8		mA

Electrical Characteristics

V^+ = +5.0V, (Note 7), unless otherwise stated

Parameter	Conditions	LM124/LM224			LM324			LM2902			Units
		Min	Typ	Max	Min	Typ	Max	Min	Typ	Max	
Input Offset Voltage	(Note 8) T_A = 25˚C		2	5		2	7		2	7	mV
Input Bias Current (Note 9)	$I_{IN(+)}$ or $I_{IN(-)}$, V_{CM} = 0V, T_A = 25˚C		45	150		45	250		45	250	nA
Input Offset Current	$I_{IN(+)}$ or $I_{IN(-)}$, V_{CM} = 0V, T_A = 25˚C		3	30		5	50		5	50	nA
Input Common-Mode Voltage Range (Note 10)	V^+ = 30V, (LM2902, V^+ = 26V), T_A = 25˚C	0		V^+–1.5	0		V^+–1.5	0		V^+–1.5	V

Electrical Characteristics (Continued)

V^+ = +5.0V, (Note 7), unless otherwise stated

Parameter		Conditions		LM124/LM224			LM324			LM2902			Units
				Min	Typ	Max	Min	Typ	Max	Min	Typ	Max	
Supply Current		Over Full Temperature Range $R_L = \infty$ On All Op Amps											mA
		V^+ = 30V (LM2902 V^+ = 26V)			1.5	3		1.5	3		1.5	3	
		V^+ = 5V			0.7	1.2		0.7	1.2		0.7	1.2	
Large Signal Voltage Gain		V^+ = 15V, $R_L \geq 2k\Omega$, (V_O = 1V to 11V), T_A = 25˚C		50	100		25	100		25	100		V/mV
Common-Mode Rejection Ratio		DC, V_{CM} = 0V to V^+ − 1.5V, T_A = 25˚C		70	85		65	85		50	70		dB
Power Supply Rejection Ratio		V^+ = 5V to 30V (LM2902, V^+ = 5V to 26V), T_A = 25˚C		65	100		65	100		50	100		dB
Amplifier-to-Amplifier Coupling (Note 11)		f = 1 kHz to 20 kHz, T_A = 25˚C (Input Referred)			−120			−120			−120		dB
Output Current	Source	V_{IN}^+ = 1V, V_{IN}^- = 0V, V^+ = 15V, V_O = 2V, T_A = 25˚C		20	40		20	40		20	40		mA
	Sink	V_{IN}^- = 1V, V_{IN}^+ = 0V, V^+ = 15V, V_O = 2V, T_A = 25˚C		10	20		10	20		10	20		mA
		V_{IN}^- = 1V, V_{IN}^+ = 0V, V^+ = 15V, V_O = 200 mV, T_A = 25˚C		12	50		12	50		12	50		µA
Short Circuit to Ground		(Note 5) V^+ = 15V, T_A = 25˚C			40	60		40	60		40	60	mA
Input Offset Voltage		(Note 8)				7			9			10	mV
V_{OS} Drift		R_S = 0Ω			7			7			7		µV/˚C
Input Offset Current		$I_{IN(+)} - I_{IN(-)}$, V_{CM} = 0V				100			150		45	200	nA
I_{OS} Drift		R_S = 0Ω			10			10			10		pA/˚C
Input Bias Current		$I_{IN(+)}$ or $I_{IN(-)}$			40	300		40	500		40	500	nA
Input Common-Mode Voltage Range (Note 10)		V^+ = +30V (LM2902, V^+ = 26V)		0		V^+–2	0		V^+–2	0		V^+–2	V
Large Signal Voltage Gain		V^+ = +15V (V_OSwing = 1V to 11V) $R_L \geq 2$ kΩ		25			15			15			V/mV
Output Voltage Swing	V_{OH}	V^+ = 30V	R_L = 2 kΩ	26			26			22			V
		(LM2902, V^+ = 26V)	R_L = 10 kΩ	27	28		27	28		23	24		
	V_{OL}	V^+ = 5V, R_L = 10 kΩ			5	20		5	20		5	100	mV
Output Current	Source	V_O = 2V	V_{IN}^+ = +1V, V_{IN}^- = 0V, V^+ = 15V	10	20		10	20		10	20		mA
	Sink		V_{IN}^- = +1V, V_{IN}^+ = 0V, V^+ = 15V	5	8		5	8		5	8		

Note 4: For operating at high temperatures, the LM324/LM324A/LM2902 must be derated based on a +125˚C maximum junction temperature and a thermal resistance of 88˚C/W which applies for the device soldered in a printed circuit board, operating in a still air ambient. The LM224/LM224A and LM124/LM124A can be derated based on a +150˚C maximum junction temperature. The dissipation is the total of all four amplifiers — use external resistors, where possible, to allow the amplifier to saturate of to reduce the power which is dissipated in the integrated circuit.

Note 5: Short circuits from the output to V^+ can cause excessive heating and eventual destruction. When considering short circuits to ground, the maximum output current is approximately 40 mA independent of the magnitude of V^+. At values of supply voltage in excess of +15V, continuous short-circuits can exceed the power dissipation ratings and cause eventual destruction. Destructive dissipation can result from simultaneous shorts on all amplifiers.

Note 6: This input current will only exist when the voltage at any of the input leads is driven negative. It is due to the collector-base junction of the input PNP transistors becoming forward biased and thereby acting as input diode clamps. In addition to this diode action, there is also lateral NPN parasitic transistor action